energies

MDPI

Review

Solar Hydrogen Fuel Generation from Wastewater—Beyond Photoelectrochemical Water Splitting: A Perspective

Sudhagar Pitchaimuthu [1,*], Kishore Sridharan [2], Sanjay Nagarajan [3], Sengeni Ananthraj [4,5], Peter Robertson [6], Moritz F. Kuehnel [7,8], Ángel Irabien [9] and Mercedes Maroto-Valer [1]

1 Research Centre for Carbon Solutions, Institute of Mechanical and Processing Engineering, School of Engineering & Physical Science, Heriot-Watt University, Edinburgh EH14 4AS, UK
2 Department of Nanoscience and Technology, School of Physical Sciences, University of Calicut, Thenhipalam 673635, India
3 Department of Chemical Engineering, University of Bath, Bath BA2 7AY, UK
4 Department of Applied Chemistry, School of Advanced Science and Engineering, Waseda University, 3-4-1 Okubo, Shinjuku-ku, Tokyo 169-8555, Japan
5 Waseda Research Institute for Science and Engineering, Waseda University, 3-4-1 Okubo, Shinjuku-ku, Tokyo 169-8555, Japan
6 School of Chemistry and Chemical Engineering, Queen's University, Belfast BT7 1NN, UK
7 Department of Chemistry, Swansea University, Singleton Park, Swansea SA2 8PP, UK
8 Fraunhofer Institute for Wind Energy Systems (IWES), Am Haupttor 4310, 06237 Leuna, Germany
9 Department of Chemical and Biomolecular Engineering (ETSIIT), University of Cantabria, Avda. los Castros, 39005 Santander, Spain
* Correspondence: s.pitchaimuthu@hw.ac.uk

Abstract: Green hydrogen—a carbon-free renewable fuel—has the capability to decarbonise a variety of sectors. The generation of green hydrogen is currently restricted to water electrolysers. The use of freshwater resources and critical raw materials, however, limits their use. Alternative water splitting methods for green hydrogen generation via photocatalysis and photoelectrocatalysis (PEC) have been explored in the past few decades; however, their commercial potential still remains unexploited due to the high hydrogen generation costs. Novel PEC-based simultaneous generation of green hydrogen and wastewater treatment/high-value product production is therefore seen as an alternative to conventional water splitting. Interestingly, the organic/inorganic pollutants in wastewater and biomass favourably act as electron donors and facilitate the dual-functional process of recovering green hydrogen while oxidising the organic matter. The generation of green hydrogen through the dual-functional PEC process opens up opportunities for a "circular economy". It further enables the end-of-life commodities to be reused, recycled and resourced for a better life-cycle design while being economically viable for commercialisation. This review brings together and critically analyses the recent trends towards simultaneous wastewater treatment/biomass reforming while generating hydrogen gas by employing the PEC technology. We have briefly discussed the technical challenges associated with the tandem PEC process, new avenues, techno-economic feasibility and future directions towards achieving net neutrality.

Keywords: photoelectrocatalysis; dual-functional photocatalysis; hydrogen generation; wastewater treatment; biomass reforming

Citation: Pitchaimuthu, S.; Sridharan, K.; Nagarajan, S.; Ananthraj, S.; Robertson, P.; Kuehnel, M.F.; Irabien, Á.; Maroto-Valer, M. Solar Hydrogen Fuel Generation from Wastewater—Beyond Photoelectrochemical Water Splitting: A Perspective. *Energies* **2022**, *15*, 7399. https://doi.org/10.3390/en15197399

Academic Editor: Kyu-Jung Chae

Received: 30 August 2022
Accepted: 1 October 2022
Published: 9 October 2022

1. Introduction

Global climate change triggering catastrophic events such as wildfires, longer periods of drought and frequent high-intensity tropical storms are attributed to global warming caused by excessive usage of fossil fuels and its associated greenhouse gas emissions. While the global energy demand continues to surge with the growing population it needs to be satisfied via alternative and sustainable green energy vectors rather than unsustainable fossil fuels [1]. The recently concluded UN climate change conference of the parties (COP26),

Glasgow (November 2021) emphasised this need for a clean energy transition. Moving away from coal and other fossil fuels especially indicates the necessity of developing low-carbon energy routes for the future [2]. In this context, green hydrogen is a promising clean energy vector due to its carbon-free emission characteristics and has the potential to replace conventional fossil fuel resources [3,4]. At present, hydrogen is mostly produced from the steam methane reforming process, commonly known as "grey hydrogen" [5]. However, this process significantly impacts the environment due to the considerable emission of CO_2 (9–12 kg CO_2/kg H_2) and is also reliant on continuous methane supply (often produced from fossil fuels) [6]. To mitigate the carbon emissions from grey hydrogen production, carbon capture and sequestration routes have been explored paving the way for "blue hydrogen".

Conversely, intermittent renewable energy resource (solar, wind, etc.)-driven hydrogen production by water splitting through electrolysis [7], photocatalysis [8], and photoelectrocatalysis [9–12], termed "green hydrogen", is gaining more attention due to its net zero emission nature. The advantage of green hydrogen produced by these techniques is its broader applicability viz. its capability to support the decarbonisation of hard-to-abate sectors such as heating, long-distance transportation and heavy industries (e.g., steel, cement, chemical) and its ability to contribute to the replacement of fossil-based materials via combined production of chemical feedstock and fertilisers for agriculture and synthetic fuels. Among these techniques, photocatalysis and photoelectrocatalysis (PEC) may be operated under natural sunlight, leading to a remarkable reduction in operating costs. Similarly, low-power LED irradiated PEC reactors are prospective devices for indoor operation [13]. Additionally, PEC has a lower system complexity than photovoltaic (PV) driven electrolysis and yields a higher overall hydrogen generation efficiency over photocatalysis [14]. Furthermore, the notably lower operating potential for water oxidation using the PEC technique than electrolysis is attractive in gaining commercial interest. Photocatalysis offers advantages such as an even lower cost and complexity due to the absence of any wiring or membrane; however, it suffers from low efficiency due to recombination and the mixing of anodic and cathodic reaction products as well as difficulties in catalyst recovery [15,16].

Regardless of the methods used for green hydrogen generation, freshwater has been used as an electrolyte in the water-splitting process; however, it is a limited critical resource of paramount significance to all known forms of life [17]. Furthermore, energy assessment studies indicate that establishing a 1 GW electricity generation facility based on PEC requires an enormous volume of (~820,000 m^3) freshwater as an electrolyte [18]. Although seawater has been proposed as an alternative electrolyte, the logistical limitations for seawater transportation and use in electrolysers (offshore) are yet to be overcome. On the contrary, using sacrificial electron donors (SED) to reduce the freshwater footprint has been proposed.

SED are compounds that can be oxidised at the anode (instead of water) to generate excess electrons that can contribute to reducing the protons obtained from water. The use of SED reduces the required applied potential for oxidation. Typical performance indicators such as the solar-to-H_2 conversion efficiency (STH) of a catalyst are boosted by suppressing the rate of recombination by the addition of various hole scavengers (SED). However, this is an economically expensive affair, as value-added platform chemicals such as alcohols, acids or sugars are typically used, and the generated green hydrogen may not even neutralise the cost of the SED. Such a process would not only add significant operating costs but is also unsustainable and negates the purpose of green hydrogen generation. On the other hand, wastewater consisting of persistent organic pollutants or waste biomass residue has been recently proposed as an SED for green hydrogen generation [19,20]. Such an alternative process is an attractive and economically feasible approach for green H_2 generation [21].

The state of the art in PEC-based green hydrogen generation focuses on novel catalytic materials for water splitting [22–29], reactor engineering [30–34], and to an extent on new SEDs [35–37]. However, the area of tandem PEC for simultaneous hydrogen generation and meaningful oxidation processes (wastewater treatment or biomass oxidation) is still

upcoming and is the main focus of this review. The conventional PEC-based wastewater treatment approach only aims to remove pollutants from water. However, when wastewater is used for the generation of green hydrogen, it paves the way for a simultaneous treatment strategy. Such an approach enables the oxidative degradation of pollutants in wastewater combined with the production of green hydrogen [38,39]. Furthermore, conventional wastewater treatment through established chemical and biological techniques is inadequate for eliminating persistent organic compounds due to their high chemical stability [40]. Even at low concentrations (ppm levels), these organic compounds have raised severe concerns owing to their capability to stimulate antimicrobial drug resistance and subsequent threat to human health due to their ability to damage cognitive functions, disrupt the endocrine system, cause reproductive disorders, and even cause cancer [41]. Therefore, addressing the complete elimination of these pollutants from wastewater is critical alongside green hydrogen generation.

It is anticipated that integrating wastewater treatment (anode) along with green hydrogen generation (cathode) via the PEC technique can lower power consumption and thereby reduce the carbon footprint of wastewater treatment plants (WWTPs). Beyond wastewater, when biomass or its derivatives are used, valuable by-products at the anode instead of oxygen can be generated [42,43]. This enables the prospects of a PEC-based biomass refinery for the simultaneous production of green hydrogen as well as value-added platform chemicals. Such a strategy reduces the water footprint, produces green energy and generates excess revenue to keep the levelised cost of hydrogen (LCH) within a desired range.

To facilitate simultaneous green hydrogen generation at the cathode and value-added product production or wastewater treatment at the anode, semiconductor (photo)electrocatalyst design and development are critical [44]. Although vital, it has to be ensured that such materials are developed based on the non-critical raw materials available locally. This would further help in maintaining the sustainability of the green hydrogen generation process and will not interfere with the critical raw material value chain. The technical challenges in photocatalysis such as particle agglomeration-induced charge recombination, poor charge separation (electrons and holes), low quantum yield, and post-recovery of the catalysts after the process hinder its commercialisation for industrial applications [15,16]. In this context, the PEC technique is capable of overcoming the aforementioned issues. Choi and co-workers reported on developing an energy and resource-recovering water treatment platform using the PEC technique [45]. Similar types of dual-functional attempts have been documented using different water pollutants and biomass. For instance, a PEC cell fabricated with dual photoelectrode (WO_3 and CuO) simultaneously performs wastewater treatment and hydrogen production [46]. Similarly, a Bi_2MoO_6 nanoparticle-decorated TiO_2 nanotube array performed conversion of benzyl alcohol to benzaldehyde along with hydrogen generation at the CuO cathode [47]. Herein, the oxidation of water pollutants or chemical species by semiconductor anode was identified as the key for initiating simultaneous reaction processes. Though the proof of concept of "simultaneous wastewater treatment and hydrogen generation" was established two decades ago [48], a poor understanding of the materials and dual-functional process required time to adapt to this route. Recent reviews on dual-functional photocatalysis/photoelectrocatalysis for simultaneous wastewater treatment and hydrogen generation shed more light on understanding this concept's importance [49,50]. However, a critical review is still necessary to understand the factors affecting PEC for simultaneous wastewater/biomass oxidation and H_2 generation. Capturing cross-sectorial coupling and system integration opportunities and the techno-economic feasibility of the dual-functional PEC process also need to be perceived. Therefore, in this review, we summarise the opportunities and challenges of a dual-functional photo/electrocatalysis process with PEC for wastewater/biomass oxidation and hydrogen generation, particularly from non-conventional feedstocks. In the first part, the important literature on wastewater treatment combined with green hydrogen generation is discussed. Then, the prospects of using biomass as an alternative

to wastewater have also been highlighted. The parameters of PEC which influence the process efficiency and yield and, finally, the techno-economics are briefly discussed.

2. Is Wastewater a Viable Feedstock for Hydrogen Generation?

Nearly 1000 km^3 of wastewater is generated every year from municipal and industrial sectors globally [51]. According to the recent report by Li et al., wastewater treatment plants (WWTPs) consume 3% of global electricity if treated with conventional technologies [52]. Considering the wastewater production of ~11 billion L/day in the UK, >2300 tons of H_2 could be produced daily theoretically (on a stoichiometric basis). This quantity is ~13 fold higher than the daily electrical energy requirements (6.34 GWh) of wastewater treatment plants in the UK. It shows the potential of wastewater for PEC hydrogen generation at WWTPs. The basic idea of PEC green hydrogen generation from wastewater is illustrated in Figure 1, wherein both wastewater treatment utilising the photogenerated holes and energy/resource recovery using the photogenerated electrons are synchronised.

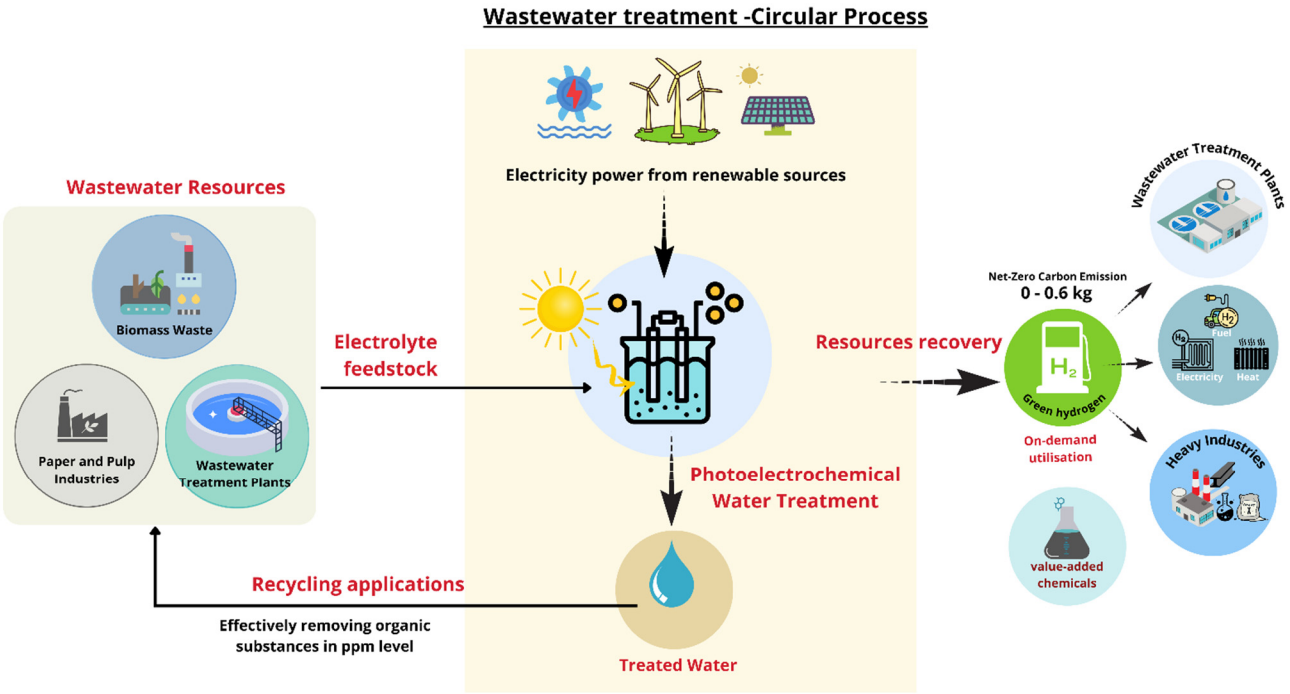

Figure 1. PEC green hydrogen generation from wastewater treatment and its utilisation.

Organic and inorganic compounds in various forms, including persistent organic pollutants, biomass, dyes and heavy metal complexes are processed in WWTPs. Unfortunately, the present WWTPs are not capable of removing these emerging pollutants and the only process capable of eliminating them are advanced oxidation processes. While common advanced oxidation processes such as photocatalysis and electrocatalysis are capable of non-specific mineralisation of these pollutants, PEC has the potential to add more value to the process. Typically, wastewater treatment is a linear process. However, the constituents of wastewater can be utilised as electrolytes for the PEC process to recover valuable resources. Therefore, simultaneous treatment of organic pollutants and resource recovery through the PEC process is a novel way forward for ensuring the circular approach of the wastewater industry.

The PEC anodic water oxidation process with fresh water is a four photohole process. In Equation (1), the by-product protons (H^+) will be transported to the cathode through a proton exchange membrane and reduced to hydrogen gas by a two-electron reduction process in Equation (2).

$$2\,H_2O\ (\text{fresh water}) + 4\,h^+ \rightarrow 4\,H^+ + O_2\ (E^0 = 1.23\ \text{V vs. RHE}) \quad (1)$$

$$2\,H^{+}+2\,e^{-} \rightarrow H_2\ (E^0 = 0\ \text{V vs. RHE}) \quad (2)$$

The energetic structure of a semiconductor photoanode thermodynamically dictates the desired redox reactions. Mainly, the semiconductor anode's valence band maximum (VBM) position is a crucial component in water pollutant oxidation. For instance, the band gap of anatase TiO_2 lies at 2.8 eV, while it is reduced to 2.3 eV under nitrogen doping [53]. Though nitrogen doping promotes the visible light PEC activity of TiO_2, doping above the optimised concentration negatively shifts the valence band position (<1.23 V vs. RHE), affecting the water oxidation performance.

Using polluted water as an electrolyte in the anode compartment instead of freshwater modifies the PEC anodic reaction. The organic molecules present in the pollutants may compete with the water oxidation process as the redox potential of pollutant oxidation differs. Water pollutants such as persistent chemicals, dyes and metal complexes or biomass can be oxidised via photoholes, $^{\bullet}OH$ radicals or other oxidants formed in solution. In a direct oxidation route in Equation (4), photoholes will produce $^{\bullet}OH$ radicals at +2.73 V vs. RHE that effectively oxidise/mineralise the water pollutants [54]. Textile dye pollutants and persistent organic pollutants (e.g., 4-chlorophenol) [44], are excellent examples of this bifunctional degradation and hydrogen production method. However, wide bandgap energy metal oxides (TiO_2, WO_3, $SrTiO_3$, etc.) are only favourable for $^{\bullet}OH$ radical generation. Unfortunately, these wide bandgap energy materials are UV light active materials and inadequate in harvesting visible light photons, unsuitable for natural sunlight-based reactors. Chemical salt (NaCl, Na_2SO_4, NaOH, KOH, etc.) is usually added for better electrolyte conductivity and scavenging photoholes effectively. Based on the salts, the $^{\bullet}OH$ radical production rate will be varied.

$$TiO_2 + h\nu \rightarrow e^{-} + h^{+} \quad (3)$$

$$h^{+} + H_2O \rightarrow {}^{\bullet}OH + H^{+} \quad (4)$$

$$h^{+} + OH^{-} \rightarrow {}^{\bullet}OH \quad (5)$$

The semiconductor crystallite phase also fixes the $^{\bullet}OH$ radical formation. The anatase/rutile mixed crystallite phase of TiO_2 showed higher $^{\bullet}OH$ radical generation than the pure anatase phase due to the reduced charge recombination rate [55]. Furthermore, the surface property of the photoanode influences the oxidation of water molecules to $^{\bullet}OH$ radicals. Nosaka et al. [56] reported that the coordination sites of the OH group of TiO_2, namely terminal OH and bridging OH groups, result in different $^{\bullet}OH$ radical production rates.

$$\equiv\text{Ti-OH} \leftrightarrow \equiv Ti^{+} + OH^{-} \quad (6)$$

$$\equiv\text{Ti-OH} + H^{+} \leftrightarrow \text{Ti-}OH_2{}^{+} \quad (7)$$

In Equations (6) and (7), the excess charge of the Ti atom of terminal OH is positive, and the positive hole prevents the attacking of the Ti–O bond of the terminal OH. It is thus not favourable for $^{\bullet}OH$ radical production. If the oxygen species in the bridging OH Equation (8) has a negative charge, it is energetically favourable to attract positive holes. The same group studied pH-dependent $^{\bullet}OH$ radical formation, which will be discussed further in the next section [57].

$$\equiv\text{Ti-OH} + h^{+} \rightarrow \equiv Ti^{+} + {}^{\bullet}OH \quad (8)$$

Figure 2 illustrates simultaneous PEC wastewater treatment/biomass oxidation (anode) and hydrogen gas production at the cathode. Note that route (I) indicates the photohole-driven direct oxidation of pollutants via $^{\bullet}OH$ radicals and two-step oxidation via in situ oxidant synthesis (active chlorine species, hydrogen peroxide, etc.). The second route (II) represents biomass waste reforming which donates oxidative electrons to the anode. Choi et al. [58] explored the crystalline phase-dependent generation of mobile

free OH radical ($^{\bullet}OH_f$) using tetramethylammonium (TMA) cation as a probe. These free OH radicals helped extend the reaction zone for mineralisation of non-adsorbing substrates from the surface to the solution bulk. Therefore, probing the crystallite phase and surface property of the photoanode controls the $^{\bullet}OH$ radical formation and thereby determines the oxidation rate.

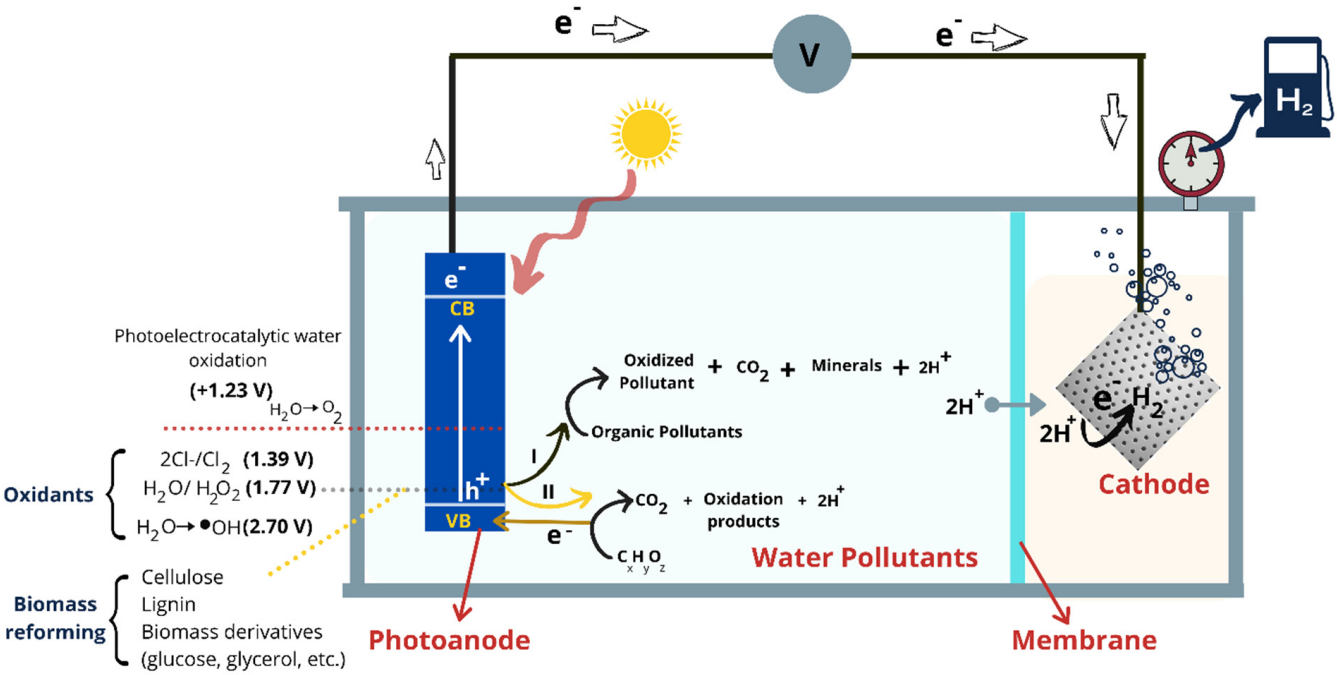

Figure 2. Schematic illustration of photoelectrocatalytic processes for simultaneous water treatment (anode) and hydrogen gas production at the cathode.

There are many PEC-driven indirect routes reported to oxidise water pollutants. Among them, the reactive chlorine species (RCS) generation and hydrogen peroxide oxidiser synthesis are upcoming routes to degrade organic contaminants and disinfect pathogens present in water [59]. It is anticipated that these PEC synthesised oxidisers are powerful in oxidising water pollutants. The generation of hypochlorous acid and hypochlorite ions are the main side reactions in the anodic production of chlorine due to the hydrolysis of dissolved chlorine in the bulk solution according to the following equations [60,61].

$$Cl_2\,(aq) + H_2O + h^+_{VB} \rightarrow Cl^-(aq) + HClO + H^+(aq) \quad (9)$$

$$h^+_{VB} + Cl^- \rightarrow Cl^{\bullet} \quad (10)$$

$$Cl^{\bullet} + Cl^- \rightarrow Cl_2{}^{-\bullet} \quad (11)$$

$$h^+_{VB} + \text{Organic} \rightarrow \text{Organic}_{\text{oxidation}} \rightarrow CO_2 \quad (12)$$

In single-compartment PEC cells, anodically generated RCS could be subsequently reduced on the cathode Equations (13)–(15), thereby lowering the production efficiency of H_2 [59].

$$HOCl + H^+ + 2\,e^- \rightarrow Cl^- + H_2O \quad (13)$$

$$Cl^{\bullet} + e^- \rightarrow Cl^- \quad (14)$$

$$Cl_2{}^{\bullet} + e^- \rightarrow 2Cl^- \quad (15)$$

Therefore, two-compartment cells separated with a proton exchange membrane are favourable for a high hydrogen generation rate by hindering the competitive reaction of RCS reduction at the cathode. Another potential oxidiser in the water pollutant treatment industry

is hydrogen peroxide. PEC anodic hydrogen peroxide generation showed high momentum in recent research using WO_3, $BiVO_4$ (pure and doped), and SnO_2 photoanodes [61–66].

$$2\ H_2O + 2\ h^+_{VB} \rightarrow H_2O_2 + 2\ H^+ + 2\ e^-\ (E^0 = +\ 1.77\ V\ vs.\ RHE) \quad (16)$$

Though the PEC hydrogen peroxide synthesis has been successfully demonstrated in lab-scale reactors, the degradation of water pollutants at a photoanode is scarce. Few reports are available on water pollutant degradation at the cathode compartment where the PEC process produced photoelectrons, a crucial component driving electrocatalytic hydrogen peroxide synthesis at the cathode [67,68]. Therefore, there is ample room to utilise the in situ synthesised PEC hydrogen peroxide for degrading organic water contaminants at the photoanode and concurrent hydrogen generation at the cathode.

The biomass residue deemed as waste from paper pulp, sugar cane industries, and agri-forest residues can also be oxidised to obtain value-added by-products alongside green hydrogen. A typical anodic reaction of the biomass reforming process is shown in Equation (17).

$$C_xH_yO_2 + H_2O \rightarrow \text{Oxidised products} + H^+ + e^-\ (\text{anode reaction}) \quad (17)$$

Currently, PEC-based biomass reforming is in its infancy and the reported literature is in the process of understanding the fundamentals behind biomass oxidation and the use of biomass as sacrificial electron donors. Biomass is a complex material and is a general terminology that is used for any organic compound that is obtained from plants or animals. Plant-derived biomass is of immense interest as it is the most abundant organic material on the earth's surface. Such biomass usually has a varying combination of cellulose, hemicellulose, and lignin interlinked to form a stable structure. Because of the recalcitrance posed by the biomass in addition to its insolubility in water and other common electrolytes, fundamental PEC studies on biomass reforming tend to use its derivatives such as mono/oligosaccharides, pentoses or lignin monomers. Glucose is accordingly a popular choice as its polymer cellulose forms the major fraction of most plant biomasses, typically >50% by dry weight [69]. Unlike cellulose, glucose is soluble in water and it is therefore easier to understand the mechanism of PEC biomass reforming using glucose as a model sacrificial electron donor. While the mechanism can be understood using glucose, obtaining it through conventional pre-treatment and saccharification methods requires a substantial operating cost. Another interesting biomass derivative is glycerol. The PEC glycerol anodic oxidation is attractive to synthesise value-added chemicals such as formic acid and dihydroxyacetone in combination with green hydrogen gas generation [70–73]. It is worth mentioning that dihydroxyacetone has been applied as an active ingredient in the sunless tanners with a very high commodity value of GBP ~108/kg compared to the price of both crude and purified glycerol of GBP <0.2/kg and GBP ~0.4/kg, respectively [44]. Interestingly, the PEC process allows probing the selectivity of the by-product ratio by tuning processing parameters of the photoanode material, the applied potential and electrolyte engineering.

Long-chain biomass-derived polymers such as cellulose or lignin are challenging to break through $^{\bullet}OH$ radicals as there are limitations related to mass transfer (bringing the biomass in slurry close to the photoelectrodes) and bulk diffusion (of $^{\bullet}OH$ radicals). Therefore, attempts to immobilise cellulose onto the photocatalyst surface for the production of green hydrogen gas have been reported [74,75]. In addition, recent research reports on PEC-based lignin reforming are also encouraging, which opens the possibilities for a broader range of value-added commodity production associated with green hydrogen generation [35,76–78]. Unlike other organic water pollutant degradation explained earlier, the biomass reforming process could contribute oxidative electrons to the anode arithmetically, which can be added with photoelectrons produced in the photoanode and promotes the overall hydrogen generation rate at the cathode.

Therefore, the PEC biomass reforming process might yield high quantum efficiency for hydrogen generation. The protons (H^+) produced from pollutant oxidation as in Equations (4), (6), (13) and (14) at the anode compartment will be transported to the cathode and reduced to hydrogen gas as in Equation (2).

3. Photoanode Choice for PEC Water Pollutant Treatment

A wide range of semiconductor materials is available for PEC water splitting and water treatment. The energetic bandgap structure of the photoanode with respect to the normal hydrogen electrode (NHE) dictates the water oxidation performance. Mainly, the valence band position of the semiconductor which is more positive than a water oxidation potential of 1.23 V NHE is suitable for oxidising pollutants via •OH radical formation. However, some organic species or biomass have a less positive oxidising potential than water. A simple example of an appropriate semiconductor PEC catalyst for •OH radical generation is TiO_2. However, TiO_2 absorbs only UV light which is only 5% of the light photons available from the solar spectrum and not ideal for outdoor applications [53]. Active chlorine species, hydrogen peroxide and SO_4^{2-} are other potential water cleaning chemicals which can be formed through PEC techniques. Figure 3 illustrates the appropriate semiconductor materials for the PEC •OH radical formation, active chlorine species/hydrogen peroxide synthesis, and biomass reforming processes. Therefore, the band structure of semiconductors and the oxidation potential of water pollutants or particular types of biomass are critical parameters for choosing the PEC materials.

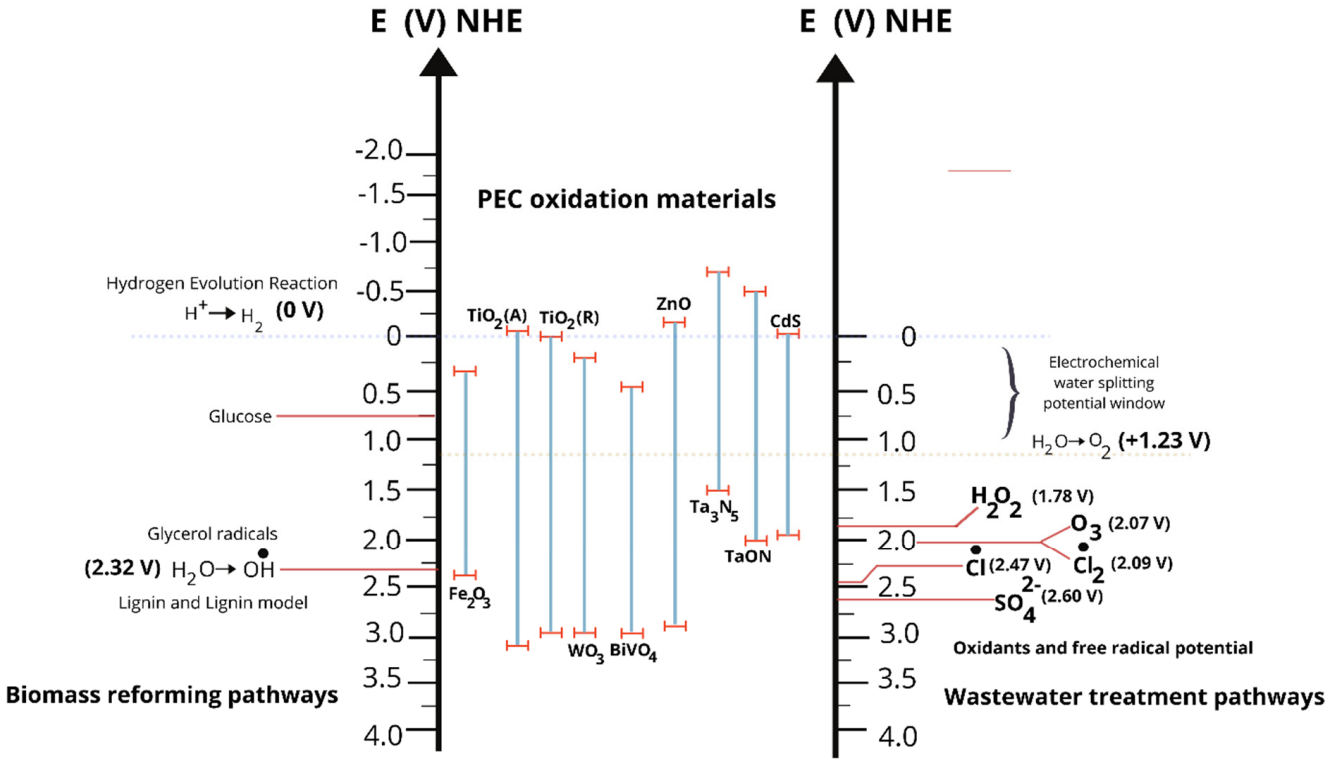

Figure 3. Bandgap energetic structure of potential semiconductors for water pollutants oxidation and biomass reforming. The redox potential of water oxidation is compared with different free radicals and oxidisers. Note that the oxidation potential values are pH dependent.

4. Fabrication of Photoelectrodes

The photoelectrode is a primary component of the PEC cells which harvests photons to the catalytic reaction sites. Unlike photocatalysis, complexity in the fabrication of photoelectrocatalyst in electrode form is challenging. For instance, coating methodologies of PEC electrodes dictate the quality of the catalyst in charge collection at the circuit and control

charge recombination kinetics at electrode/electrolyte interfaces. Typically, semiconductor photoelectrocatalyst materials are deposited either via physical or chemical coating technology as depicted in Figure 4. In general, the semiconductor thin films are coated onto a charge collector (substrate-conducting glass, sheet or mesh metals, etc.) through a direct or indirect approach. In the direct method, the semiconductor catalyst is deposited through the atom-by-atom approach (bottom-up). Sputtering or thermal evaporation are good examples of preparing uniform, robust catalyst coating at ambient temperature and pressure through an indirect approach [79]. In these techniques, energetic particles of plasma or gas hit the surface of a target solid (metals or alloys) where the atoms from the target vapourise into ions and get deposited onto the substrate to form a layer with a few nanometres to a few micrometres thick, called a "thin film". In the case of the atomic layer deposition technique, the metal precursor chemicals are used as the starting material for synthesizing semiconductor catalyst coating [80–82]. This technique is mainly used for extremely thin layer deposition at sub-nanometre to a few nanometre scales (1–2 nm). A recent review on catalyst design by the ALD technique helps in understanding the process further [83]. Both sputtering and ALD routes are vacuum-based techniques which are relatively more expensive than chemical routes. Alternatively, the spray coating route is a cheaper option that offers a wide choice of substrates without the requirement of a vacuum. Precursors dispersed in an appropriate solvent (aqueous or non-aqueous) are employed as starting materials, which are atomized as aerosol particles and coated on the substrate [84]. Modified spray techniques such as electrospray, thermal, ultrasonic or plasma-assisted spray provide a highly adhesive robust coating to conventional pneumatic sprayers. Electrodeposition is another promising approach to fabricating semiconductor films. The respective metals of semiconductor catalysts are dissolved in an ionic electrolyte and can be translated into a coating by applying electric potential in the circuit. The wet chemical routes such as dip coating and spin coating are simple compared with the abovementioned techniques [85,86]. However, reproducibility and large-scale deposition still remain a major challenge. Each technique has its own merits and challenges. For example, few catalysts required a high-temperature process, conducting property or vacuum environment which restricts the substrate choice. The previously synthesized semiconductor catalyst in powder form or suspended in liquid media can be coated on any desired substrate. In this two-stage method, a suitable binder will be often applied as glue to stick the semiconductor catalyst on the substrate surface. Later, the binder will be selectively removed by the annealing process or UV curing process [87]. Doctor blade or screen printing techniques are widely used to coat the homogenous catalyst inks or paste on the substrate [88].

The film integrity on the substrate is a critical issue that determines the electrode stability [89]. Particularly the thickness of the catalyst dictates its sustainability in the electrolyte environment. Mostly films with thin coatings (less than 1 micron) are much better than thick films (>1 micron). A modified electrode architecture such as mesoporous, 3-D foam allows higher loading of PEC material without sacrificing charge collection or charge recombination issues. More care should be taken when choosing the substrate and adopting the appropriate coating methodology while the electrode is being fabricated for wastewater treatment processes for avoiding secondary pollution due to leaching out of the electrode material from the coating.

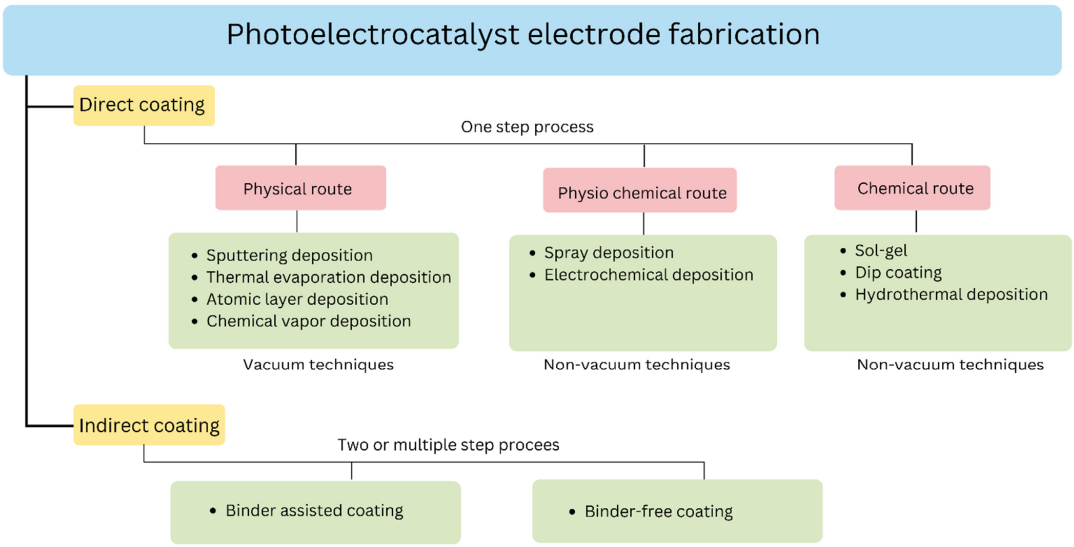

Figure 4. Classification of coating techniques for photoelectrode fabrication.

5. Advantages of Photoelectrochemical Reactors for Simultaneous Reactions

Compared to PEC, dual-functional photocatalysis using nanostructured semiconductor particles as photocatalysts is not suitable for practical applications due to various challenges. For instance, compared to the PEC technique, the recovery of the nanostructured photocatalyst particles from the slurry containing the organic pollutant in wastewater after the photocatalytic reaction to avoid secondary pollution is challenging and demands additional efforts. The hindrance of visible light absorption by the individual photocatalyst particles in the presence of coloured pollutants in opaque wastewater or a biomass slurry can lead to poor quantum yields. In contrast, the PEC process enables direct irradiation of the photoelectrode surface and averts the issues encountered in photocatalysis. Recombination of the photogenerated electrons and holes in the semiconductor photocatalyst cannot be easily controlled, whereas in PEC, the use of an external bias leads to the effective separation of electrons and holes to the cathode and anode, respectively and can significantly enhance the photodegradation efficiency and H_2 yield. Further, in the dual-functional photocatalysis reaction, H_2 generated is not pure and contains CO_2 as an organic pollutant degradation by-product. This can be avoided in PEC since H_2 is produced at the cathode and is well isolated from the anode wherein the oxidation of the organic pollutants takes place. Unlike semiconductor photocatalysts, PEC offers the possibility of running independent reactions and the choice of degrading two or more pollutants simultaneously [90–95]. Note that the photocatalysis technique has few merits compared with PEC, i.e., less ohmic resistance, and effective inter-particle reactions which supports the kinetics and mobility of participatory ions in the reactions [96].

Although the usage of twin reactors for dual functional photocatalysis application was demonstrated by Li et al. [97] using two different nanostructured semiconductor photocatalysts, the solar-to-H_2 conversion efficiency (STH) was still very low for practical applications and the produced H_2 was not pure and contained reaction by-products. Furthermore, the feasibility to adopt secondary power sources such as photovoltaic panels, wind power, etc. is another added advantage of using the PEC technique for dual-functional photocatalysis applications [98]. Some of the recent reports on the dual-functional PEC system for the degradation of pollutants including SO_2 and CO_2 and the simultaneous hydrogen generation are listed in Table 1. Interestingly, dual-functional PEC systems have also been used for the generation of H_2O_2 while removing SO_2 [99], and for the treatment of biomass and plastics [72,100]. However, the surface chemistry of the electrodes in the electrolyte and the stability of the photoelectrodes are of significant concern and are discussed in detail in the following sections.

Table 1. Dual-functional PEC for oxidation of waste with simultaneous generation of hydrogen reported in the literature under simulated solar light.

Feedstock	PEC Type	Photoanode	Cathode	Applied Potential	Electrolyte	Light Source and Intensity	By-Products	Hydrogen Generation	Ref.
Glucose (0.33 mM)	Double compartment cell	Bi_2WO_6	Pt wire	0.9 V vs. SHE	Na_2SO_4 0.1 M phosphate-buffered solution, pH = 7	100 mW cm^{-2}	Negligible amount of CO_2	3.05 µmol h^{-1} cm^{-2}	[101]
Glucose (2.5 mM)	Single compartment cell	Cu_2O/TiO_2	Pt wire	0.7 V vs. Ag/AgCl	1 M NaOH aqueous	100 mW cm^{-2}	Not studied	122 µmol h^{-1} cm^{-2}	[84]
Glycerol	Single compartment cell	CoNiFe-LDH co-catalyst decorated anodised Ta_3N_5 nanotube array	Pt plate	1.2 V RHE	Electrolyte: 1.0 M NaOH, pH = 13.6.	500 W xenon arc lamp 100 mW cm^{-2}	Formic acid	60 µ.mL/h.cm^2	[71]
Glycerol	Two-compartment cell	$BiVO_4$	Pt plate	1.2 V RHE	0.5 M Na_2SO_4 at various pH (adding NaOH and H_2SO_4) with and without glycerol.	-	Dihydroxyacetone Formic acid	No hydrogen gas measurements	[72]
Glycerol	Single compartment cell	$BiVO_4$	Pt	1.2 V RHE	0.1 M $Na_2B_4O_7$ (NaBi, pH 9.4) aqueous solution including various glycerol concentrations, i.e., 0, 0.1, 0.5, 1.0, 2.0, and 3.0 M	-	Dihydroxyacetone Formic acid	30 µ.mL/h.cm^2	[102]
Wastewater and pollutants									
Ibuprofen, Benzophenone, and Carbamazepine (2 ppm)	Single compartment cell (100 mL)	Bilayer BiOI/BiVO4	Pt foil	1.0 V vs. Ag/AgCl	1.5 mM Na_2SO_3, pH = 7	100 mW cm^{-2}	Complete mineralisation	75 µmol h^{-1} cm^{-2}	[103]
SO_2 (500 ppm)	Single compartment cell	Inverse opal Mo doped $BiVO_4$	Pt wire	0.7 V vs. Ag/AgCl	0.1 mM NaOH, pH = 7	100 mW cm^{-2}	Na_2SO_3	60 µmol h^{-1} cm^{-2}	[104]
SO_2 (1000 ppm) and CO_2	Two compartment cell (50 mL) separated by proton exchange membrane	$BiVO_4$	Cu-In alloy	0.92 V vs. Ag/AgCl	0.2 M $NaHCO_3$, pH = 7	100 mW cm^{-2}	CO and HCOOH	3.45 µmol h^{-1} cm^{-2}	[92]
SO_2	Two compartment cell separated by an anion exchange membrane	Pd/Nickel Foam	NiO/Ni/Nickel Foam	1.3 V vs. Ag/AgCl	5mM KOH, pH = 12 at cathode and 50 mM $(NH_4)_2SO_3$ in 0.5 M $(NH_4)_2SO_4$ solution in anode, pH = 8	100 mW cm^{-2}	NH_3	0.25 mmol h^{-1} cm^{-2}	[105]
Carbamazepine (CBZ)	Two-compartment cell separated by Nafion membrane	Cl doped TiO_2	H-Ag	1.5 V vs. Ag/AgCl	Anode electrolyte: 100 mL 0.1 M Na_2SO_4 containing 5 mgL^{-1} CBZ. Cathode electrolyte: 90 mL 0.1 M $KHCO_3$ solution. The cathode chamber was purged with CO2 gas for 0.5 h before the experiment.	100 mW cm^{-2}	Anode: minerals and CO_2 Cathode: CO, HCOOH	41.7 µmol h^{-1} cm^{-2}	[94]

Table 1. *Cont.*

Feedstock	PEC Type	Photoanode	Cathode	Applied Potential	Electrolyte	Light Source and Intensity	By-Products	Hydrogen Generation	Ref.
Methyl orange dye	Double compartment cell	$CdSe/TiO_2$	Pt sheet	0.5 V vs. Ag/AgCl	0.2 M Na_2S	100 mW cm^{-2}—with 400 nm UV filter	Minerals and CO_2	0.43 mmol.cm^{-2}	[106]
Reactive Black 5 azo (RB5) dye	Two-compartment cell	$Ti/TiO_2/WO_3$	Pt mesh	1.0 V vs. Ag/AgCl	Anode electrolyte: $7.0 \times 10-5$ mol L^{-1} concentration of RB5 dye in 0.1 mol L^{-1} Na2SO4 at pH 6 (anodic compartment) and pH 4 (cathodic compartment).	300-W Xe arc lamp with a cutoff filter ($\lambda > 420$ nm) 15 mW cm^{-2}	alkylsulfonyl phenolic compounds	0.45 mL/h.cm^2	[59]
Rhodamine B	Single compartment cell	Photoanode: W doped TiO_2	Pt	Not mentioned	Electrolyte: Na_2S (0.1 M) and Na_2SO_3(0.02 M)		CO_2 and minerals	25 µ.ml/h.cm^2	[10]

This work mainly provides representative examples of semiconductor PEC materials performing simultaneous water treatment and hydrogen generation. However, we advise further reading of the previous review and research reports in which the fundamental properties of various PEC materials and their influencing properties for water splitting performance are discussed in detail [107–116].

6. Electrolyte Engineering

The electrolyte environment has an extreme influence on the diffusion of pollutants treated, transport of the charge carriers and surface kinetics of redox reactions at the photoanode [117]. Notably, the pH of the electrolyte in the PEC system impacts the mass transport of pollutants towards the photoanode and mainly dictates its surface functional property. Increasing the pH above a particular range can hinder pollutant photodegradation due to altering the photoanode surface. It hampers the hydrogen generation efficiency at the cathode due to the drop in the number of protons produced. For instance, Zheng et al. [99] found that the initial electrolyte pH affected PEC degradation of benzophenone-3 when they demonstrated the simultaneous degradation of pharmaceutical and personal care products and hydrogen evolution over a bilayer BiOI/$BiVO_4$ photoanode. At an optimum pH of 6, a degradation efficiency of 94.7% for benzophenone-3 was reported after 90 min. Nonetheless, the efficiency decreased when the pH was increased further. The declining photodegradation efficiency with the increasing pH was attributed to the change of surface potential of $BiVO_4$ at different pH values, which in turn was caused by the random distribution of Na_2SO_3 in the electrolyte. For the BiOI/$BiVO_4$ photoanode, the point of zero charge (pH_{pzc}) was found to be around pH 4.1, and its surface is negatively charged at pH > 4.1 which favoured the absorption of benzophenone-3 and accelerated its photodegradation. Similarly, the existence of sulfite as HSO_3^- below pH 7.1 favoured photodegradation as it is less basic and does not compete with benzophenone-3. However, when the pH is increased to >9.5, the existence of SO_3^{2-} makes it difficult for the benzophenone-3 to reach the photoanode. On the other hand, the band bending and charge transfer characteristics of the photoanode also rely on the redox-inert potential window of the electrolyte. Tayyebi et al. reported an enhanced photodegradation of methylene blue dye molecules in a PEC system with a $BiVO_4$ photoanode when the electrolyte pH was higher than 6.5. Interestingly, at pH 9.5 the $BiVO_4$ surface was found to become negative due to deprotonation which triggered higher band bending that resulted in higher PEC performance as a consequence of an efficient electron-hole separation. However, regardless of the influence of pH, the photocurrent density is often higher with back-illumination of the electrode compared to front-illumination due to the higher absorption depth, wherein most of the incident light gets absorbed by the $BiVO_4$ close to the FTO region resulting in the easy transfer of the electrons to the external circuit towards the counter electrode for H_2 generation reaction [87,118]. In this regard, the pH of the electrolyte as well as the light illumination direction on the anode are needed to be carefully optimised for obtaining enhanced PEC efficiency in the photodegradation of organic pollutants and H_2 generation. It should be noted that the pH of the electrolyte is a trade-off between the photoanode surface functionality, pollutants adsorption and analyte distribution. Further, the chemical additives added to the electrolyte viz. NaCl, Na_2SO_3, Na_2SO_4, etc., are capable of generating free radicals and stabilising them at optimum pH conditions, which can boost the dual-functional photocatalytic degradation and H_2 generation efficiency.

Ambrosio et al. [119] analysed the effect of pH on the alignment of redox levels at the $BiVO_4$(010)–water interface by combining the calculated band alignment with the acid-base chemistry of the $BiVO_4$(010) surface as shown in the Pourbiax diagram (Figure 5), wherein the electrode/electrolyte interface was theoretically distinguished as three regions of pH for understanding the underlying mechanism of the water oxidation reaction. As shown in Figure 4, the ε_v^{SHE} was calculated at the PBE (dotted line) and at the PBE0(α) level as a function of pH, while the redox levels for dehydrogenation of water molecules (red dashed line) and oxidation of hydroxyl ion (blue dotted line) were calculated based on ab

initio molecular dynamics [120]. The results of their study were nearly in resonance with the experimental results discussed previously [92,99]. Surface oxidation during the PEC process could affect the water oxidation performance of non-oxides for different reasons, including (a) enhanced charge recombination because of the introduction of electron/hole recombination centres, (b) reduced light transmittance due to light absorption and scattering by the newly formed oxide coating, and (c) affect the photocharge carrier transfer efficiency from the photoanode to the electrolyte [121]. Recently, Li et al. [122] explored the influence of surface oxidation of the Ta_3N_5 photoanode on the hole transfer rate in various oxidising solutions. They found that N–O replacement by surface oxidation at the Ta_3N_5 surface increases the carrier recombination rate near the surface and, to a lesser degree, reduces the interfacial hole transfer rate. The necessary hole transfer at electrode/electrolyte interfaces leads to photocorrosion and is a drop in water oxidation performance. We will discuss this issue in the next section.

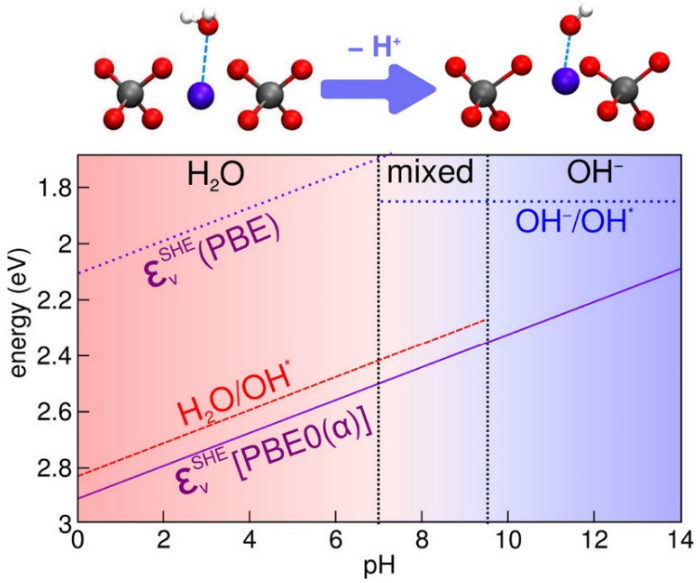

Figure 5. The pH dependence of the band energy levels of a $BiVO_4$ photoanode. Reprinted from ref. [119]. Figure adopted with permission from ACS publishers.

7. Photo/Electro Corrosion of Electrodes

Managing long-term operation without a detrimental drop in process performance is required for the industrial implementation of PEC as a sustainable technology. In this view, a critical aspect is the stability of the photoelectrode against photo/electrochemical corrosion. Nandjou et al. [123] reported a detailed kinetic model for the photostability of the semiconductor electrodes against the oxygen evolution reaction (OER) and the anodic photocorrosion reaction (APR). The report states that the photostability of electrodes is dependent on reaction rates and hole concentration. Importantly, self-oxidation of semiconductors is a primary issue for photocorrosion. Chen et al. [124] explained that self-oxidation depends on the energy levels of semiconductors. Figure 6a schematically illustrates the self-oxidation process at a photoanode. In general, the semiconductor can be stable, based on the hole oxidation, if its oxidation potential (ϕ^{ox}) is lower than either $E(O_2/H_2O)$ or its valence band maximum (VBM). Considering the example of a WO_3 photoanode, Figure 6b depicts different electrolytes' decomposition potentials and compares them with the thermodynamic potentials of water splitting and the band position of WO_3 [125]. It demonstrates that the (estimated) oxidation potential of $HClO_4$ is close to the valence band, and therefore the photoanode with this electrolyte is relatively stable against oxidation. However, in the presence of Cl^- anions, the decomposition potentials of complex-forming electrolytes (CH_3SO_3H) are in a similar range as the decomposition potential of WO_3. Note that every semiconductor has its self-oxidation potential. Therefore,

one should carefully estimate the oxidation potential of organic pollutants and the energetic structure of the photoanode before treating wastewater. Significantly, pH and electrolyte additives could vary the oxidation potential of the pollutants [126]. The Pourbaix diagram can be used to assess the stability of a material against corrosion based on the pH and applied potential. Guo et al. [127] summarised the oxidation potential of 202 inorganic materials and gave an overview of stable photoanodes for water pollutant treatment.

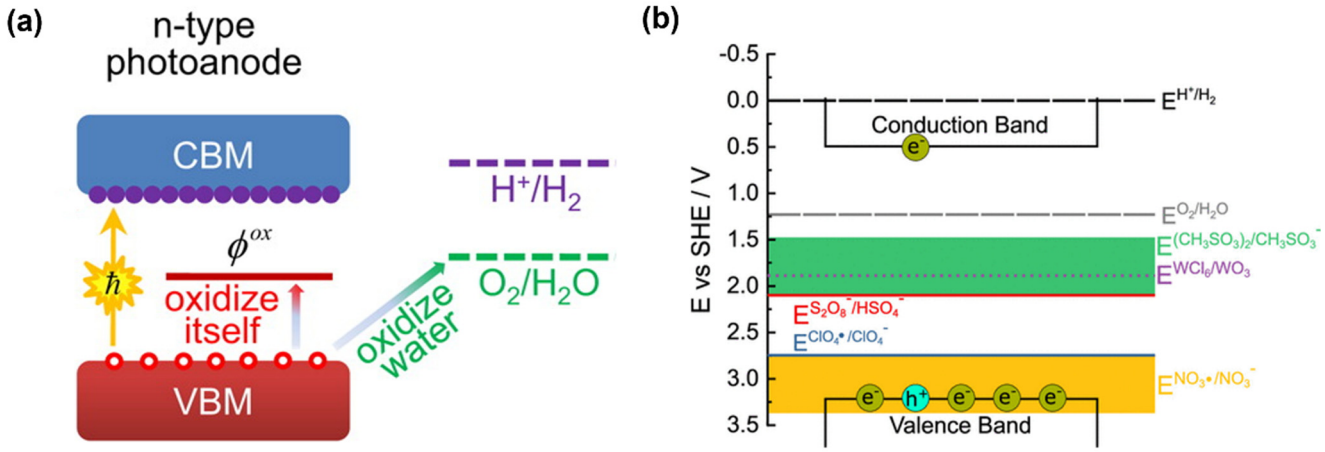

Figure 6. Schematic illustration of (**a**) the band alignment of the n-type photoanode semiconductors relative to the water redox potentials and ϕ^{ox} shows the oxidation potential of the photoanode in aqueous solution, and (**b**) different energy levels of electrolyte redox pairs concerning the valence and conduction band of WO_3. Figure 6a,b has been reused with permission from ref. [124,125], Copyright American Chemical Society.

In situ experimental tools using X-ray, spectroelectrochemistry [128–131], or electrochemical techniques [132,133], explored the corrosion events at the photoanode/electrolyte interface. For instance, the valence band maximum of $BiVO_4$ located at ~2.6 V vs. RHE is favourable for water oxidation, but its self-oxidation potential ϕ^{ox} = 1.3 V vs. RHE is slightly more positive than its water oxidation potential. Hence, if the applied potential in the PEC reaction increases above 1.3 V vs. RHE, $BiVO_4$ could undergo photoanodic decomposition. Yao et al. [5] examined the stability of $BiVO_4$ in PEC water oxidation. After photoirradiation, they found the dissolution of V in the electrolyte, while Bi remained on the anode as solid bismuth oxide (Bi_2O_3, Bi_4O_7). Bismuth oxide accumulation on the anode surface was advantageous as it led to passivation from further degradation. The co-catalyst decoration or passivation layer coating on an anode surface can modify the redox potential required for pollutant oxidation. Compared to the water oxidation process, organic water pollutants are favourable for photohole scavenging, which helps to stabilise the photoanode. It was observed in $BiVO_4$ that corrosion could happen in highly alkaline conditions due to the kinetically favourable oxidation of hydroxyl ions, whereas in acidic conditions, it favoured water oxidation [119]. Zhang et al. [134] studied the in situ dissolution behaviour of a $BiVO_4$ photoanode in various pH-buffered electrolytes and found that the PEC dissolution rates were sensitive to the surface chemistry and morphology. Therefore, photoelectrochemical corrosion is the most significant issue for photoanodes immersed in liquid electrolytes or water pollutants.

8. Techno-Economic Analysis

Sacrificial electron donor-mediated PEC processes have been increasing recently. Intensive research on this topic has led to the development of interesting materials that could be used as photoelectrodes (TiO_2, ZnO, WO_3, Fe_2O_3, $BiVO_4$, CdS, CdSe, PbS, Ta_3N_5, C_3N_4, CuO, $SrTiO_3$, MoS_2) for efficient harvesting of light energy into chemical energy (H_2) [91–97,135–141]. Though the materials aspect of PEC, including bandgap engineering and surface morphology, are important pillars to improving the solar-to-hydrogen efficiency

(STH) and advancing the field, the technology readiness level (TRL) for PEC H_2 remains low (TRL 2-3). This is mainly because of the poor stability of the electrodes, challenges upon the scaling-up of such systems and its inability to meet the techno-economics efficiently. Especially, the design of stable large-scale photoelectrodes is a pressing limitation. For instance, Ahmed and Dincer point out that it is necessary to achieve 10% STH with at least a 10-year photoelectrode lifetime to be commercially viable [142]. The techno-economics are greatly affected by a few broad factors, namely (i) STH, (ii) reactor configuration and (iii) fluid handling. The common point of agreement within the literature is that STH improvement is an effective means to lower the cost of H_2. Sathre et al. [18] reported that the gas and liquid handling in PEC-based H_2 production systems do not influence the cost of H_2 production significantly. Additionally, with the fundamentals of PEC H_2 generation well established, a paradigm shift in focus towards the engineering aspects of PEC to address the challenges in STH improvement and reactor optimisation is required. This is the only possible way to improve the TRL of PEC H_2 systems towards a commercial reality. For instance, Pinaud et al. [143] from their technoeconomic simulations pointed out that it may be possible to produce H_2 from water splitting economically (GBP 1.2–7.7/kg H_2) within the price guidelines set by the United States Department of Energy (GBP 1.5–2.9/kg H_2). Although a number of assumptions were in place to arrive at this LCH, it was pointed out that PEC would lead the way to achieving these costs over photocatalysis. Hypothetical simulations along the line of work by Pinaud and co-authors have also been performed by other researchers who arrived at various values of LCH for a range of different technologies, as shown in Table 2. Similarly, most reports suggest PEC as the way forward towards commercialisation and some suggest that the PV-powered electrolysers are favourable. The problem however with electrolysers is the requirement of fresh water for their operation and the use of critical raw material catalysts [144].

Table 2. Overview of simulated LCH reported in the literature. TPD refers to tonnes per day.

Technology	Simulated H_2 Plant Capacity	LCH (£/kg H_2)	Ref.
Photocatalysis PEC	1 TPD	1.2–2.4 3–7.7	[143]
PV-E PEC	0.01 TPD	4.5–8.9 6.8–8.4	[145]
PEC	610 TPD	-	[18]
PV-E PEC	10 TPD	4.6 6.2	[146]

Nevertheless, novel strategies to enhance renewable H_2 production should be brought forward, and PEC is flexible in adapting to such a strategy compared to its water-splitting counterparts. For instance, wastewater-based PEC H_2 production would facilitate both wastewater treatment as well as H_2 generation and would fit the circular economy framework by utilising waste as a resource for renewable fuel production and to lower the freshwater load. While this body of work is on the rise [20,147], lignin and biomass photoreforming are also receiving immense attention recently [42,75,148,149]. Initial pointers presented by Rumayor et al. for instance provide LCA-based evidence that biomass photoreforming is a sustainable method to generate green hydrogen [150]. Their analysis showed that even for shorter lifetimes and lower productivities, biomass photoreforming could be similar in terms of global warming potential to water electrolysis with low CO_2 emissions. While the environmental and social factors are favourable, detailed techno-economics (at least an order of estimate analysis) in this aspect are an immediate need. Currently, techno-economic analyses are available for freshwater-based PEC H_2 production systems. It can serve as a base case, and investigating the feasibility of a waste stream operated PEC for the dual purposes of waste treatment and H_2 generation is the crucial next step. The baseline lab-scale data are used for simulating large-scale H_2 costing; however, this is

challenging. Therefore, it is essential to understand how scaling-up works and its impact on performance. To facilitate this, a stepwise scaling-up approach to PEC H_2 systems is required, wherein a lab-scale system (cm^3) can be first scaled to a pilot system (m^3) followed by an industrial unit (100 m^3). Such a systemic approach would help take into account the drop in performance and efficiencies between scales. Empirical equations accounting for the drop in performance with scale can then be used, followed by simulations of PEC H_2 costing. This approach would eliminate the overestimation of H_2 gate prices and help optimise the systems to mitigate the drop in performance.

9. Conclusions

Simultaneous PEC wastewater treatment/biomass oxidation at a photoanode and hydrogen generation at the cathode is a cost-saving route, but it requires more understanding of the electrode/pollutant interface. Not all water pollutants may disperse in water and thus require a co-solvent, which, however, might alter the redox potential. Therefore, more attention is needed for each stage of the electrolyte process. Furthermore, after dispersing the pollutants in water, the pH environment might be varied. The modified pH and redox potential may lead to photocorrosion of the photoanode. New anode architectures with doping, creating oxygen vacancies, assembling co-catalysts, and passivation layer coatings will help reduce the applied energy input and prevent the photocorrosion of the photoanode. As discussed, the organic water pollutant oxidation pathways can be varied for each pollutant and semiconductor photoanode. The effective charge carrier transfers, i.e., photoholes to the electrolyte and electrons to anode, dictate the pollutant degradation or biomass reforming efficiency and quantum yield of hydrogen production rate per hour/cm^2. However, critical components such as band positions, surface functionality of the photoanode, the pH environment and additives in the electrolyte directly affect the photocharge carrier separation. Therefore, more attention is required to these parameters. The taxonomy analysis of green hydrogen should be carried out for wastewater pollutants as feedstock. The transport of the wastewater should be taken into account to avoid hidden costs. PEC for this case can be utilised as a decentralised technology for waste remediation as well as energy generation. Furthermore, a critical understanding of the underlying mechanisms through electronic structure methods is needed to optimise experimental conditions to prevent corrosion. Note that this review mainly focuses on the prospectus of the photoanode, and electrolyte engineering towards hydrogen generation and less discussion on formed products/intermediates. Thus, further knowledge is required to understand the potential-dependent identification of the formed products/intermediates.

Author Contributions: S.P. conceived the idea, and all the authors contributed to the content, proof reading, and editing. All authors have read and agreed to the published version of the manuscript.

Funding: This research received no external funding. The APC was funded by Heriot-Watt University (Start-up grant).

Institutional Review Board Statement: Not applicable.

Informed Consent Statement: Not applicable.

Data Availability Statement: Not applicable.

Acknowledgments: The lead author S.P. thanks the School of Engineering and Physical Sciences, Heriot-Watt University for providing start-up grant support.

Conflicts of Interest: The authors declare no conflict of interest.

References

1. Hoffert, M.I. Farewell to Fossil Fuels? *Science* **2010**, *329*, 1292–1294. [CrossRef] [PubMed]
2. COP26: Green Technologies Could Turn the Tide. *Nat. Rev. Mater.* **2021**, *6*, 959. [CrossRef]
3. Staffell, I.; Scamman, D.; Abad, A.V.; Balcombe, P.; Dodds, P.E.; Ekins, P.; Shah, N.; Ward, K.R. The Role of Hydrogen and Fuel Cells in the Global Energy System. *Energy Environ. Sci.* **2019**, *12*, 463–491. [CrossRef]

4. Hanley, E.S.; Deane, J.P.; Gallachóir, B.P.Ó. The Role of Hydrogen in Low Carbon Energy Futures–A Review of Existing Perspectives. *Renew. Sustain. Energy Rev.* **2018**, *82*, 3027–3045. [CrossRef]
5. Yao, X.; Zhao, X.; Hu, J.; Xie, H.; Wang, D.; Cao, X.; Zhang, Z.; Huang, Y.; Chen, Z.; Sritharan, T. The Self-Passivation Mechanism in Degradation of $BiVO_4$ Photoanode. *iScience* **2019**, *19*, 976–985. [CrossRef] [PubMed]
6. Sun, P.; Young, B.; Elgowainy, A.; Lu, Z.; Wang, M.; Morelli, B.; Hawkins, T. Criteria Air Pollutants and Greenhouse Gas Emissions from Hydrogen Production in U.S. Steam Methane Reforming Facilities. *Environ. Sci. Technol.* **2019**, *53*, 7103–7113. [CrossRef] [PubMed]
7. Dotan, H.; Landman, A.; Sheehan, S.W.; Malviya, K.D.; Shter, G.E.; Grave, D.A.; Arzi, Z.; Yehudai, N.; Halabi, M.; Gal, N.; et al. Decoupled Hydrogen and Oxygen Evolution by a Two-Step Electrochemical–chemical Cycle for Efficient Overall Water Splitting. *Nat. Energy* **2019**, *4*, 786–795. [CrossRef]
8. Takata, T.; Jiang, J.; Sakata, Y.; Nakabayashi, M.; Shibata, N.; Nandal, V.; Seki, K.; Hisatomi, T.; Domen, K. Photocatalytic Water Splitting with a Quantum Efficiency of Almost Unity. *Nature* **2020**, *581*, 411–414. [CrossRef]
9. Walter, M.G.; Warren, E.L.; McKone, J.R.; Boettcher, S.W.; Mi, Q.; Santori, E.A.; Lewis, N.S. Solar Water Splitting Cells. *Chem. Rev.* **2010**, *110*, 6446–6473. [CrossRef]
10. Gong, J.; Pu, W.; Yang, C.; Zhang, J. Novel One-Step Preparation of Tungsten Loaded TiO2 Nanotube Arrays with Enhanced Photoelectrocatalytic Activity for Pollutant Degradation and Hydrogen Production. *Catal. Commun.* **2013**, *36*, 89–93. [CrossRef]
11. Roger, I.; Shipman, M.A.; Symes, M.D. Earth-Abundant Catalysts for Electrochemical and Photoelectrochemical Water Splitting. *Nat. Rev. Chem.* **2017**, *1*, 3. [CrossRef]
12. Landman, A.; Dotan, H.; Shter, G.E.; Wullenkord, M.; Houaijia, A.; Maljusch, A.; Grader, G.S.; Rothschild, A. Photoelectrochemical Water Splitting in Separate Oxygen and Hydrogen Cells. *Nat. Mater.* **2017**, *16*, 646–651. [CrossRef] [PubMed]
13. Tokode, O.; Prabhu, R.; Lawton, L.A.; Robertson, P.K.J. UV LED Sources for Heterogeneous Photocatalysis. *Handb. Environ. Chem.* **2014**, *35*, 159–179. [CrossRef]
14. Kim, J.H.; Hansora, D.; Sharma, P.; Jang, J.-W.; Lee, J.S. Toward Practical Solar Hydrogen Production—An Artificial Photosynthetic Leaf-to-Farm Challenge. *Chem. Soc. Rev.* **2019**, *48*, 1908–1971. [CrossRef] [PubMed]
15. Nandy, S.; Savant, S.A.; Haussener, S. Prospects and Challenges in Designing Photocatalytic Particle Suspension Reactors for Solar Fuel Processing. *Chem. Sci.* **2021**, *12*, 9866–9884. [CrossRef] [PubMed]
16. Wang, Q.; Domen, K. Particulate Photocatalysts for Light-Driven Water Splitting: Mechanisms, Challenges, and Design Strategies. *Chem. Rev.* **2020**, *120*, 919–985. [CrossRef]
17. Jones, B.; Davies, K.R.; Allan, M.G.; Anantharaj, S.; Mabbett, I.; Watson, T.; Durrant, J.R.; Kuehnel, M.F.; Pitchaimuthu, S. Photoelectrochemical Concurrent Hydrogen Generation and Heavy Metal Recovery from Polluted Acidic Mine Water. *Sustain. Energy Fuels* **2021**, *5*, 3084–3091. [CrossRef]
18. Sathre, R.; Scown, C.D.; Morrow, W.R.; Stevens, J.C.; Sharp, I.D.; Ager, J.W.; Walczak, K.; Houle, F.A.; Greenblatt, J.B. Life-Cycle Net Energy Assessment of Large-Scale Hydrogen Production via Photoelectrochemical Water Splitting. *Energy Environ. Sci.* **2014**, *7*, 3264–3278. [CrossRef]
19. Jiang, H.; Wang, X.; Li, C.; Gu, D.; Jiang, T.; Nie, C.; Yuan, D.; Wu, H.; Wang, B. An Alternative Electron-Donor and Highly Thermo-Assisted Strategy for Solar-Driven Water Splitting Redox Chemistry towards Efficient Hydrogen Production plus Effective Wastewater Treatment. *Renew. Energy* **2021**, *176*, 388–401. [CrossRef]
20. Rioja-Cabanillas, A.; Valdesueiro, D.; Fernández-Ibáñez, P.; Byrne, J.A. Hydrogen from Wastewater by Photocatalytic and Photoelectrochemical Treatment. *J. Phys. Energy* **2020**, *3*, 012006. [CrossRef]
21. Wu, Z.; Zhao, G.; Zhang, Y.; Liu, J.; Zhang, Y.; Shi, H. A Solar-Driven Photocatalytic Fuel Cell with Dual Photoelectrode for Simultaneous Wastewater Treatment and Hydrogen Production. *J. Mater. Chem. A* **2015**, *3*, 3416–3424. [CrossRef]
22. Bian, H.; Li, D.; Yan, J.; Liu, S. (Frank) Perovskite – A Wonder Catalyst for Solar Hydrogen Production. *J. Energy Chem.* **2021**, *57*, 325–340. [CrossRef]
23. Yalavarthi, R.; Henrotte, O.; Minguzzi, A.; Ghigna, P.; Grave, D.A.; Naldoni, A. In Situ Characterizations of Photoelectrochemical Cells for Solar Fuels and Chemicals. *MRS Energy Sustain.* **2020**, *7*, 37. [CrossRef]
24. Moniz, S.J.A.; Shevlin, S.A.; Martin, D.J.; Guo, Z.X.; Tang, J. Visible-Light Driven Heterojunction Photocatalysts for Water Splitting—A Critical Review. *Energy Environ. Sci.* **2015**, *8*, 731–759. [CrossRef]
25. Yang, J.; Wang, D.; Han, H.; Li, C. Roles of Cocatalysts in Photocatalysis and Photoelectrocatalysis. *Acc. Chem. Res.* **2013**, *46*, 1900–1909. [CrossRef] [PubMed]
26. Kim, T.W.; Choi, K.S. Nanoporous BiVO4 Photoanodes with Dual-Layer Oxygen Evolution Catalysts for Solar Water Splitting. *Science* **2014**, *343*, 990–994. [CrossRef] [PubMed]
27. Wang, D.; Li, R.; Zhu, J.; Shi, J.; Han, J.; Zong, X.; Li, C. Photocatalytic Water Oxidation on $BiVO_4$ with the Electrocatalyst as an Oxidation Cocatalyst: Essential Relations between Electrocatalyst and Photocatalyst. *J. Phys. Chem. C* **2012**, *116*, 5082–5089. [CrossRef]
28. Wang, Y.; Vogel, A.; Sachs, M.; Sprick, R.S.; Wilbraham, L.; Moniz, S.J.A.; Godin, R.; Zwijnenburg, M.A.; Durrant, J.R.; Cooper, A.I.; et al. Current Understanding and Challenges of Solar-Driven Hydrogen Generation Using Polymeric Photocatalysts. *Nat. Energy* **2019**, *4*, 746–760. [CrossRef]
29. Chen, S.; Takata, T.; Domen, K. Particulate Photocatalysts for Overall Water Splitting. *Nat. Rev. Mater.* **2017**, *2*, 17050. [CrossRef]

30. Kelly, N.A.; Gibson, T.L. Design and Characterization of a Robust Photoelectrochemical Device to Generate Hydrogen Using Solar Water Splitting. *Int. J. Hydrogen Energy* **2006**, *31*, 1658–1673. [CrossRef]
31. Jacobsson, T.J.; Fjällström, V.; Sahlberg, M.; Edoff, M.; Edvinsson, T. A Monolithic Device for Solar Water Splitting Based on Series Interconnected Thin Film Absorbers Reaching over 10% Solar-to-Hydrogen Efficiency. *Energy Environ. Sci.* **2013**, *6*, 3676–3683. [CrossRef]
32. Tembhurne, S.; Nandjou, F.; Haussener, S. A Thermally Synergistic Photo-Electrochemical Hydrogen Generator Operating under Concentrated Solar Irradiation. *Nat. Energy* **2019**, *4*, 399–407. [CrossRef]
33. Varadhan, P.; Fu, H.C.; Kao, Y.C.; Horng, R.H.; He, J.H. An Efficient and Stable Photoelectrochemical System with 9% Solar-to-Hydrogen Conversion Efficiency via InGaP/GaAs Double Junction. *Nat. Commun.* **2019**, *10*, 5282. [CrossRef] [PubMed]
34. Guo, S.; Li, X.; Li, J.; Wei, B. Boosting Photocatalytic Hydrogen Production from Water by Photothermally Induced Biphase Systems. *Nat. Commun.* **2021**, *12*, 1343. [CrossRef] [PubMed]
35. Schneider, J.; Bahnemann, D.W. Undesired Role of Sacrificial Reagents in Photocatalysis. *J. Phys. Chem. Lett.* **2013**, *4*, 3479–3483. [CrossRef]
36. King, J.; Chuang, S.S.C. Photoelectrochemical Conversion of Lignin to Hydrogen: Lignin as an Electron Donor. *Catal. Commun.* **2021**, *149*, 106219. [CrossRef]
37. Pellegrin, Y.; Odobel, F. Sacrificial Electron Donor Reagents for Solar Fuel Production. *Comptes Rendus Chim.* **2017**, *20*, 283–295. [CrossRef]
38. Pan, D.; Xiao, S.; Chen, X.; Li, R.; Cao, Y.; Zhang, D.; Pu, S.; Li, Z.; Li, G.; Li, H. Efficient Photocatalytic Fuel Cell via Simultaneous Visible-Photoelectrocatalytic Degradation and Electricity Generation on a Porous Coral-like WO3/W Photoelectrode. *Environ. Sci. Technol.* **2019**, *53*, 3697–3706. [CrossRef]
39. Divyapriya, G.; Singh, S.; Martínez-Huitle, C.A.; Scaria, J.; Karim, A.V.; Nidheesh, P.V. Treatment of Real Wastewater by Photoelectrochemical Methods: An Overview. *Chemosphere* **2021**, *276*, 130188. [CrossRef]
40. Shenoy, S.; Ahmed, S.; Lo, I.M.C.; Singh, S.; Sridharan, K. Rapid Sonochemical Synthesis of Copper Doped ZnO Grafted on Graphene as a Multi-Component Hierarchically Structured Visible-Light-Driven Photocatalyst. *Mater. Res. Bull.* **2021**, *140*, 111290. [CrossRef]
41. Shenoy, S.; Sridharan, K. Bismuth Oxybromide Nanoplates Embedded on Activated Charcoal as Effective Visible Light Driven Photocatalyst. *Chem. Phys. Lett.* **2020**, *749*, 137435. [CrossRef]
42. Liu, X.; Wei, W.; Ni, B. Photocatalytic and Photoelectrochemical Reforming of Biomass. In *Solar-to-Chemical Conversion*; Wiley Online Library: Hoboken, NJ, USA, 2021.
43. Lu, X.; Xie, S.; Yang, H.; Tong, Y.; Ji, H. Photoelectrochemical Hydrogen Production from Biomass Derivatives and Water. *Chem. Soc. Rev.* **2014**, *43*, 7581–7593. [CrossRef] [PubMed]
44. Sridharan, K.; Shenoy, S.; Girish Kumar, S.; Terashima, C.; Fujishima, A.; Pitchaimuthu, S. Advanced Two-Dimensional Heterojunction Photocatalysts of Stoichiometric and Non-Stoichiometric Bismuth Oxyhalides with Graphitic Carbon Nitride for Sustainable Energy and Environmental Applications. *Catalyst* **2021**, *11*, 426. [CrossRef]
45. Koo, M.S.; Cho, K.; Yoon, J.; Choi, W. Photoelectrochemical Degradation of Organic Compounds Coupled with Molecular Hydrogen Generation Using Electrochromic TiO_2 Nanotube Arrays. *Environ. Sci. Technol.* **2017**, *51*, 6590–6598. [CrossRef]
46. Zhou, Z.; Wu, Z.; Xu, Q.; Zhao, G. A Solar-Charged Photoelectrochemical Wastewater Fuel Cell for Efficient and Sustainable Hydrogen Production. *J. Mater. Chem. A* **2017**, *5*, 25450–25459. [CrossRef]
47. Zhou, Z.; Xie, Y.N.; Zhu, W.; Zhao, H.; Yang, N.; Zhao, G. Selective Photoelectrocatalytic Tuning of Benzyl Alcohol to Benzaldehyde for Enhanced Hydrogen Production. *Appl. Catal. B Environ.* **2021**, *286*, 119868. [CrossRef]
48. Hashimoto, K.; Kawai, T.; Sakata, T. Photocatalytic Reactions of Hydrocarbons and Fossil Fuels with Water. Hydrogen Production and Oxidation. *J. Phys. Chem.* **2002**, *88*, 4083–4088. [CrossRef]
49. Jeon, T.H.; Koo, M.S.; Kim, H.; Choi, W. Dual-Functional Photocatalytic and Photoelectrocatalytic Systems for Energy- and Resource-Recovering Water Treatment. *ACS Catal.* **2018**, *8*, 11542–11563. [CrossRef]
50. Kampouri, S.; Stylianou, K.C. Dual-Functional Photocatalysis for Simultaneous Hydrogen Production and Oxidation of Organic Substances. *ACS Catal.* **2019**, *9*, 4247–4270. [CrossRef]
51. Lu, L.; Guest, J.S.; Peters, C.A.; Zhu, X.; Rau, G.H.; Ren, Z.J. Wastewater Treatment for Carbon Capture and Utilization. *Nat. Sustain.* **2018**, *1*, 750–758. [CrossRef]
52. Li, W.W.; Yu, H.Q.; Rittmann, B.E. Chemistry: Reuse Water Pollutants. *Nature* **2015**, *528*, 29–31. [CrossRef] [PubMed]
53. Kumar, S.G.; Devi, L.G. Review on Modified TiO_2 Photocatalysis under UV/Visible Light: Selected Results and Related Mechanisms on Interfacial Charge Carrier Transfer Dynamics. *J. Phys. Chem. A* **2011**, *115*, 13211–13241. [CrossRef] [PubMed]
54. Wardman, P. Reduction Potentials of One-Electron Couples Involving Free Radicals in Aqueous Solution. *J. Phys. Chem. Ref. Data* **2009**, *18*, 1637. [CrossRef]
55. Tryba, B.; Toyoda, M.; Morawski, A.W.; Nonaka, R.; Inagaki, M. Photocatalytic Activity and OH Radical Formation on TiO_2 in the Relation to Crystallinity. *Appl. Catal. B Environ.* **2007**, *71*, 163–168. [CrossRef]
56. Nosaka, Y.; Nosaka, A. Understanding Hydroxyl Radical (•OH) Generation Processes in Photocatalysis. *ACS Energy Lett.* **2016**, *1*, 356–359. [CrossRef]
57. Nakabayashi, Y.; Nosaka, Y. The PH Dependence of OH Radical Formation in Photo-Electrochemical Water Oxidation with Rutile TiO_2 Single Crystals. *Phys. Chem. Chem. Phys.* **2015**, *17*, 30570–30576. [CrossRef]

58. Hwang, J.Y.; Moon, G.H.; Kim, B.; Tachikawa, T.; Majima, T.; Hong, S.; Cho, K.; Kim, W.; Choi, W. Crystal Phase-Dependent Generation of Mobile OH Radicals on TiO_2: Revisiting the Photocatalytic Oxidation Mechanism of Anatase and Rutile. *Appl. Catal. B Environ.* **2021**, *286*, 119905. [CrossRef]
59. Koo, M.S.; Chen, X.; Cho, K.; An, T.; Choi, W. In Situ Photoelectrochemical Chloride Activation Using a WO3 Electrode for Oxidative Treatment with Simultaneous H_2 Evolution under Visible Light. *Environ. Sci. Technol.* **2019**, *53*, 9926–9936. [CrossRef]
60. Kusmierek, E. Semiconductor Electrode Materials Applied in Photoelectrocatalytic Wastewater Treatment—An Overview. *Catalyst* **2020**, *10*, 439. [CrossRef]
61. Wenderich, K.; Kwak, W.; Grimm, A.; Kramer, G.J.; Mul, G.; Mei, B. Industrial Feasibility of Anodic Hydrogen Peroxide Production through Photoelectrochemical Water Splitting: A Techno-Economic Analysis. *Sustain. Energy Fuels* **2020**, *4*, 3143–3156. [CrossRef]
62. Liu, J.; Zou, Y.; Jin, B.; Zhang, K.; Park, J.H. Hydrogen Peroxide Production from Solar Water Oxidation. *ACS Energy Lett.* **2019**, *4*, 3018–3027. [CrossRef]
63. Zhang, K.; Liu, J.; Wang, L.; Jin, B.; Yang, X.; Zhang, S.; Park, J.H. Near-Complete Suppression of Oxygen Evolution for Photoelectrochemical H_2O Oxidative H_2O_2 Synthesis. *J. Am. Chem. Soc.* **2020**, *142*, 8641–8648. [CrossRef] [PubMed]
64. Fuku, K.; Miyase, Y.; Miseki, Y.; Funaki, T.; Gunji, T.; Sayama, K. Photoelectrochemical Hydrogen Peroxide Production from Water on a WO_3/$BiVO_4$ Photoanode and from O_2 on an Au Cathode Without External Bias. *Chem.–An Asian J.* **2017**, *12*, 1111–1119. [CrossRef] [PubMed]
65. Xue, Y.; Wang, Y.; Pan, Z.; Sayama, K. Electrochemical and Photoelectrochemical Water Oxidation for Hydrogen Peroxide Production. *Angew. Chemie Int. Ed.* **2021**, *60*, 10469–10480. [CrossRef] [PubMed]
66. Jeon, T.H.; Kim, B.; Kim, C.; Xia, C.; Wang, H.; Alvarez, P.J.J.; Choi, W. Solar Photoelectrochemical Synthesis of Electrolyte-Free H_2O_2 Aqueous Solution without Needing Electrical Bias and H_2. *Energy Environ. Sci.* **2021**, *14*, 3110–3119. [CrossRef]
67. Zong, X.; Chen, H.; Seger, B.; Pedersen, T.; Dargusch, M.S.; McFarland, E.W.; Li, C.; Wang, L. Selective Production of Hydrogen Peroxide and Oxidation of Hydrogen Sulfide in an Unbiased Solar Photoelectrochemical Cell. *Energy Environ. Sci.* **2014**, *7*, 3347–3351. [CrossRef]
68. Jeon, T.H.; Kim, H.; Kim, H.; Choi, W. Highly Durable Photoelectrochemical H_2O_2 Production via Dual Photoanode and Cathode Processes under Solar Simulating and External Bias-Free Conditions. *Energy Environ. Sci.* **2020**, *13*, 1730–1742. [CrossRef]
69. Isikgor, F.H.; Becer, C.R. Lignocellulosic Biomass: A Sustainable Platform for the Production of Bio-Based Chemicals and Polymers. *Polym. Chem.* **2015**, *6*, 4497–4559. [CrossRef]
70. Tang, R.; Wang, L.; Zhang, Z.; Yang, W.; Xu, H.; Kheradmand, A.; Jiang, Y.; Zheng, R.; Huang, J. Fabrication of MOFs' Derivatives Assisted Perovskite Nanocrystal on TiO_2 Photoanode for Photoelectrochemical Glycerol Oxidation with Simultaneous Hydrogen Production. *Appl. Catal. B Environ.* **2021**, *296*, 120382. [CrossRef]
71. Wang, Q.; Ma, X.; Wu, P.; Li, B.; Zhang, L.; Shi, J. CoNiFe-LDHs Decorated Ta_3N_5 Nanotube Array Photoanode for Remarkably Enhanced Photoelectrochemical Glycerol Conversion Coupled with Hydrogen Generation. *Nano Energy* **2021**, *89*, 106326. [CrossRef]
72. Liu, D.; Liu, J.-C.; Cai, W.; Ma, J.; Yang, H.B.; Xiao, H.; Li, J.; Xiong, Y.; Huang, Y.; Liu, B. Selective Photoelectrochemical Oxidation of Glycerol to High Value-Added Dihydroxyacetone. *Nat. Commun.* **2019**, *10*, 1779. [CrossRef] [PubMed]
73. Bashiri, R.; Mohamed, N.M.; Fai Kait, C.; Sufian, S.; Khatani, M. Enhanced Hydrogen Production over Incorporated Cu and Ni into Titania Photocatalyst in Glycerol-Based Photoelectrochemical Cell: Effect of Total Metal Loading and Calcination Temperature. *Int. J. Hydrogen Energy* **2017**, *42*, 9553–9566. [CrossRef]
74. Zhang, G.; Ni, C.; Huang, X.; Welgamage, A.; Lawton, L.A.; Robertson, P.K.J.; Irvine, J.T.S. Simultaneous Cellulose Conversion and Hydrogen Production Assisted by Cellulose Decomposition under UV-Light Photocatalysis. *Chem. Commun.* **2016**, *52*, 1673–1676. [CrossRef]
75. Chang, C.; Skillen, N.; Nagarajan, S.; Ralphs, K.; Irvine, J.T.S.; Lawton, L.; Robertson, P.K.J. Using Cellulose Polymorphs for Enhanced Hydrogen Production from Photocatalytic Reforming. *Sustain. Energy Fuels* **2019**, *3*, 1971–1975. [CrossRef]
76. Li, T.; Mo, J.Y.; Weekes, D.M.; Dettelbach, K.E.; Jansonius, R.P.; Sammis, G.M.; Berlinguette, C.P. Photoelectrochemical Decomposition of Lignin Model Compound on a $BiVO_4$ Photoanode. *ChemSusChem* **2020**, *13*, 3622–3626. [CrossRef] [PubMed]
77. Ko, M.; Pham, L.T.M.; Sa, Y.J.; Woo, J.; Nguyen, T.V.T.; Kim, J.H.; Oh, D.; Sharma, P.; Ryu, J.; Shin, T.J.; et al. Unassisted Solar Lignin Valorisation Using a Compartmented Photo-Electro-Biochemical Cell. *Nat. Commun.* **2019**, *10*, 5123. [CrossRef] [PubMed]
78. Wang, D.; Lee, S.H.; Han, S.; Kim, J.; Trang, N.V.T.; Kim, K.; Choi, E.-G.; Boonmongkolras, P.; Lee, Y.W.; Shin, B.; et al. Lignin-Fueled Photoelectrochemical Platform for Light-Driven Redox Biotransformation. *Green Chem.* **2020**, *22*, 5151–5160. [CrossRef]
79. Choi, G.J.; Jung, H.; Kim, D.H.; Sohn, Y.; Gwag, J.S. Photoelectrocatalytic Effect of Unbalanced RF Magnetron Sputtered TiO_2 Thin Film on ITO-Coated Patterned SiO_2 Nanocone Arrays. *Catal. Sci. Technol.* **2018**, *8*, 898–906. [CrossRef]
80. Eswar, N.K.R.; Singh, S.A.; Heo, J. Atomic Layer Deposited Photocatalysts: Comprehensive Review on Viable Fabrication Routes and Reactor Design Approaches for Photo-Mediated Redox Reactions. *J. Mater. Chem. A* **2019**, *7*, 17703–17734. [CrossRef]
81. Ng, S.; Zazpe, R.; Rodriguez-Pereira, J.; Michalička, J.; Macak, J.M.; Pumera, M. Atomic Layer Deposition of Photoelectrocatalytic Material on 3D-Printed Nanocarbon Structures. *J. Mater. Chem. A* **2021**, *9*, 11405–11414. [CrossRef]
82. Najafi, M.; Ahmadi, R.; Sham, T.K.; Salimi, A. Electrochemical Atomic Layer Deposition of Cadmium Telluride for Pt Decoration: Application as Novel Photoelectrocatalyst for Hydrogen Evolution Reaction. *Electrochim. Acta* **2019**, *321*, 134651. [CrossRef]

83. Oneill, B.J.; Jackson, D.H.K.; Lee, J.; Canlas, C.; Stair, P.C.; Marshall, C.L.; Elam, J.W.; Kuech, T.F.; Dumesic, J.A.; Huber, G.W. Catalyst Design with Atomic Layer Deposition. *ACS Catal.* **2015**, *5*, 1804–1825. [CrossRef]
84. Devadoss, A.; Sudhagar, P.; Ravidhas, C.; Hishinuma, R.; Terashima, C.; Nakata, K.; Kondo, T.; Shitanda, I.; Yuasa, M.; Fujishima, A. Simultaneous Glucose Sensing and Biohydrogen Evolution from Direct Photoelectrocatalytic Glucose Oxidation on Robust Cu_2O-TiO_2 Electrodes. *Phys. Chem. Chem. Phys.* **2014**, *16*, 21237–21242. [CrossRef] [PubMed]
85. Sahoo, P.; Sharma, A.; Padhan, S.; Thangavel, R. Cu Doped NiO Thin Film Photocathodes for Enhanced PEC Performance. *Superlattices Microstruct.* **2021**, *159*, 107050. [CrossRef]
86. Kyesmen, P.I.; Nombona, N.; Diale, M. Influence of Coating Techniques on the Optical and Structural Properties of Hematite Thin Films. *Surf. Interfaces* **2019**, *17*, 100384. [CrossRef]
87. Choi, J.; Sudhagar, P.; Kim, J.H.; Kwon, J.; Kim, J.; Terashima, C.; Fujishima, A.; Song, T.; Paik, U. WO_3/W:$BiVO_4$/$BiVO_4$ Graded Photoabsorber Electrode for Enhanced Photoelectrocatalytic Solar Light Driven Water Oxidation. *Phys. Chem. Chem. Phys.* **2017**, *19*, 4648–4655. [CrossRef]
88. Shi, X.; Jeong, H.; Oh, S.J.; Ma, M.; Zhang, K.; Kwon, J.; Choi, I.T.; Choi, I.Y.; Kim, H.K.; Kim, J.K.; et al. Unassisted Photoelectrochemical Water Splitting Exceeding 7% Solar-to-Hydrogen Conversion Efficiency Using Photon Recycling. *Nat. Commun.* **2016**, *7*, 11943. [CrossRef]
89. Tan, J.; Kang, B.; Kim, K.; Kang, D.; Lee, H.; Ma, S.; Jang, G.; Lee, H.; Moon, J. Hydrogel Protection Strategy to Stabilize Water-Splitting Photoelectrodes. *Nat. Energy* **2022**, *7*, 537–547. [CrossRef]
90. Liu, S.-S.; Xing, Q.-J.; Chen, Y.; Zhu, M.; Jiang, X.-H.; Wu, S.-H.; Dai, W.; Zou, J.-P. Photoelectrochemical Degradation of Organic Pollutants Using BiOBr Anode Coupled with Simultaneous CO_2 Reduction to Liquid Fuels via CuO Cathode. *ACS Sustain. Chem. Eng.* **2018**, *7*, 1250–1259. [CrossRef]
91. Sahara, G.; Kumagai, H.; Maeda, K.; Kaeffer, N.; Artero, V.; Higashi, M.; Abe, R.; Ishitani, O. Photoelectrochemical Reduction of CO_2 Coupled to Water Oxidation Using a Photocathode with a Ru(II)–Re(I) Complex Photocatalyst and a CoOx/TaON Photoanode. *J. Am. Chem. Soc.* **2016**, *138*, 14152–14158. [CrossRef]
92. Li, K.; Han, J.; Yang, Y.; Wang, T.; Feng, Y.; Ajmal, S.; Liu, Y.; Deng, Y.; Tahir, M.A.; Zhang, L. Simultaneous SO_2 Removal and CO_2 Reduction in a Nano-$BiVO_4$ | Cu-In Nanoalloy Photoelectrochemical Cell. *Chem. Eng. J.* **2019**, *355*, 11–21. [CrossRef]
93. Kalamaras, E.; Maroto-Valer, M.M.; Shao, M.; Xuan, J.; Wang, H. Solar Carbon Fuel via Photoelectrochemistry. *Catal. Today* **2018**, *317*, 56–75. [CrossRef]
94. Wang, D.; He, Y.; Zhong, N.; He, Z.; Shen, Y.; Zeng, T.; Lu, X.; Ma, J.; Song, S. In Situ Chloride-Mediated Synthesis of TiO_2 Thin Film Photoanode with Enhanced Photoelectrochemical Activity for Carbamazepine Oxidation Coupled with Simultaneous Cathodic H_2 Production and CO_2 Conversion to Fuels. *J. Hazard. Mater.* **2021**, *410*, 124563. [CrossRef] [PubMed]
95. Rather, R.A.; Lo, I.M.C. Photoelectrochemical Sewage Treatment by a Multifunctional G-C_3N_4/Ag/AgCl/$BiVO_4$ Photoanode for the Simultaneous Degradation of Emerging Pollutants and Hydrogen Production, and the Disinfection of *E. coli*. *Water Res.* **2020**, *168*, 115166. [CrossRef]
96. Maeda, K. Photocatalytic Water Splitting Using Semiconductor Particles: History and Recent Developments. *J. Photochem. Photobiol. C Photochem. Rev.* **2011**, *12*, 237–268. [CrossRef]
97. Li, D.; Yu, J.C.C.; Nguyen, V.H.; Wu, J.C.S.; Wang, X. A Dual-Function Photocatalytic System for Simultaneous Separating Hydrogen from Water Splitting and Photocatalytic Degradation of Phenol in a Twin-Reactor. *Appl. Catal. B Environ.* **2018**, *239*, 268–279. [CrossRef]
98. Segev, G.; Beeman, J.W.; Greenblatt, J.B.; Sharp, I.D. Hybrid Photoelectrochemical and Photovoltaic Cells for Simultaneous Production of Chemical Fuels and Electrical Power. *Nat. Mater.* **2018**, *17*, 1115–1121. [CrossRef]
99. Mei, X.; Bai, J.; Chen, S.; Zhou, M.; Jiang, P.; Zhou, C.; Fang, F.; Zhang, Y.; Li, J.; Long, M.; et al. Efficient SO_2 Removal and Highly Synergistic H_2O_2 Production Based on a Novel Dual-Function Photoelectrocatalytic System. *Environ. Sci. Technol.* **2020**, *54*, 11515–11525. [CrossRef]
100. Wu, Y.-H.; Kuznetsov, D.A.; Pflug, N.C.; Fedorov, A.; Müller, C.R. Solar-Driven Valorisation of Glycerol on $BiVO_4$ Photoanodes: Effect of Co-Catalyst and Reaction Media on Reaction Selectivity. *J. Mater. Chem. A* **2021**, *9*, 6252–6260. [CrossRef]
101. Madriz, L.; Tatá, J.; Carvajal, D.; Núñez, O.; Scharifker, B.R.; Mostany, J.; Borrás, C.; Cabrerizo, F.M.; Vargas, R. Photocatalysis and Photoelectrochemical Glucose Oxidation on Bi_2WO_6: Conditions for the Concomitant H_2 Production. *Renew. Energy* **2020**, *152*, 974–983. [CrossRef]
102. Huang, L.W.; Vo, T.G.; Chiang, C.Y. Converting Glycerol Aqueous Solution to Hydrogen Energy and Dihydroxyacetone by the BiVO4 Photoelectrochemical Cell. *Electrochim. Acta* **2019**, *322*, 134725. [CrossRef]
103. Zheng, Z.; He, J.; Dong, C.; Lo, I.M.C. Photoelectrochemical Sewage Treatment by Sulfite Activation over an Optimized $BiVO_4$ Photoanode to Simultaneously Promote PPCPs Degradation, H_2 Evolution and *E. Coli* Disinfection. *Chem. Eng. J.* **2021**, *419*, 129418. [CrossRef]
104. Han, J.; Cheng, H.; Zhang, L.; Fu, H.; Chen, J. Trash to Treasure: Use Flue Gas SO_2 to Produce H_2 via a Photoelectrochemical Process. *Chem. Eng. J.* **2018**, *335*, 231–235. [CrossRef]
105. Márquez-Montes, R.A.; Kawashima, K.; Vo, K.M.; Chávez-Flores, D.; Collins-Martínez, V.H.; Mullins, C.B.; Ramos-Sánchez, V.H. Simultaneous Sulfite Electrolysis and Hydrogen Production Using Ni Foam-Based Three-Dimensional Electrodes. *Environ. Sci. Technol.* **2020**, *54*, 12511–12520. [CrossRef]

106. Wang, W.; Li, F.; Zhang, D.; Leung, D.Y.C.; Li, G. Photoelectrocatalytic Hydrogen Generation and Simultaneous Degradation of Organic Pollutant via CdSe/TiO_2 Nanotube Arrays. *Appl. Surf. Sci.* **2016**, *362*, 490–497. [CrossRef]
107. Tan, H.L.; Abdi, F.F.; Ng, Y.H. Heterogeneous Photocatalysts: An Overview of Classic and Modern Approaches for Optical, Electronic, and Charge Dynamics Evaluation. *Chem. Soc. Rev.* **2019**, *48*, 1255–1271. [CrossRef]
108. Wu, H.; Zhang, D.; Lei, B.X.; Liu, Z.Q. Metal Oxide Based Photoelectrodes in Photoelectrocatalysis: Advances and Challenges. *Chempluschem* **2022**, *87*, e202200097. [CrossRef]
109. He, Y.; Hamann, T.; Wang, D. Thin Film Photoelectrodes for Solar Water Splitting. *Chem. Soc. Rev.* **2019**, *48*, 2182–2215. [CrossRef]
110. Zhong, S.; Xi, Y.; Chen, Q.; Chen, J.; Bai, S. Bridge Engineering in Photocatalysis and Photoelectrocatalysis. *Nanoscale* **2020**, *12*, 5764–5791. [CrossRef]
111. Melchionna, M.; Fornasiero, P. Updates on the Roadmap for Photocatalysis. *ACS Catal.* **2020**, *10*, 5493–5501. [CrossRef]
112. Lianos, P. Review of Recent Trends in Photoelectrocatalytic Conversion of Solar Energy to Electricity and Hydrogen. *Appl. Catal. B Environ.* **2017**, *210*, 235–254. [CrossRef]
113. Takanabe, K. Photocatalytic Water Splitting: Quantitative Approaches toward Photocatalyst by Design. *ACS Catal.* **2017**, *7*, 8006–8022. [CrossRef]
114. Mehtab, A.; Ahmed, J.; Alshehri, S.M.; Mao, Y.; Ahmad, T. Rare Earth Doped Metal Oxide Nanoparticles for Photocatalysis: A Perspective. *Nanotechnology* **2022**, *33*, 142001. [CrossRef] [PubMed]
115. Mehtab, A.; Alshehri, S.M.; Ahmad, T. Photocatalytic and Photoelectrocatalytic Water Splitting by Porous G-C_3N_4 Nanosheets for Hydrogen Generation. *ACS Appl. Nano Mater.* **2022**, *5*, 12656–12665. [CrossRef]
116. Ali, S.A.; Ahmad, T. Chemical Strategies in Molybdenum Based Chalcogenides Nanostructures for Photocatalysis. *Int. J. Hydrogen Energy* **2022**, *47*, 29255–29283. [CrossRef]
117. Huang, X.; Li, Y.; Gao, X.; Xue, Q.; Zhang, R.; Gao, Y.; Han, Z.; Shao, M. The Effect of the Photochemical Environment on Photoanodes for Photoelectrochemical Water Splitting. *Dalt. Trans.* **2020**, *49*, 12338–12344. [CrossRef]
118. Tayyebi, A.; Soltani, T.; Lee, B.K. Effect of PH on Photocatalytic and Photoelectrochemical (PEC) Properties of Monoclinic Bismuth Vanadate. *J. Colloid Interface Sci.* **2019**, *534*, 37–46. [CrossRef]
119. Ambrosio, F.; Wiktor, J.; Pasquarello, A. PH-Dependent Catalytic Reaction Pathway for Water Splitting at the $BiVO_4$–Water Interface from the Band Alignment. *ACS Energy Lett.* **2018**, *3*, 829–834. [CrossRef]
120. Ambrosio, F.; Miceli, G.; Pasquarello, A. Redox Levels in Aqueous Solution: Effect of van Der Waals Interactions and Hybrid Functionals. *J. Chem. Phys.* **2015**, *143*, 244508. [CrossRef]
121. Giménez, S.; Bisquert, J. *Photoelectrochemical Solar Fuel Production: From Basic Principles to Advanced Devices*; Springer: Berlin/Heidelberg, Germany, 2016; pp. 1–559. [CrossRef]
122. Li, K.; Miao, B.; Fa, W.; Chen, R.; Jin, J.; Bevan, K.H.; Wang, D. Evolution of Surface Oxidation on Ta_3N_5 as Probed by a Photoelectrochemical Method. *ACS Appl. Mater. Interfaces* **2021**, *13*, 17420–17428. [CrossRef]
123. Nandjou, F.; Haussener, S. Kinetic Competition between Water-Splitting and Photocorrosion Reactions in Photoelectrochemical Devices. *ChemSusChem* **2019**, *12*, 1984–1994. [CrossRef] [PubMed]
124. Chen, S.; Wang, L.-W. Thermodynamic Oxidation and Reduction Potentials of Photocatalytic Semiconductors in Aqueous Solution. *Chem. Mater.* **2012**, *24*, 3659–3666. [CrossRef]
125. Knöppel, J.; Kormányos, A.; Mayerhöfer, B.; Hofer, A.; Bierling, M.; Bachmann, J.; Thiele, S.; Cherevko, S. Photocorrosion of WO3 Photoanodes in Different Electrolytes. *ACS Phys. Chem. Au* **2021**, *1*, 6–13. [CrossRef]
126. Fekete, M.; Riedel, W.; Patti, A.F.; Spiccia, L. Photoelectrochemical Water Oxidation by Screen Printed ZnO Nanoparticle Films: Effect of PH on Catalytic Activity and Stability. *Nanoscale* **2014**, *6*, 7585–7593. [CrossRef]
127. Guo, L.-J.; Luo, J.-W.; He, T.; Wei, S.-H.; Li, S.-S. Photocorrosion-Limited Maximum Efficiency of Solar Photoelectrochemical Water Splitting. *Phys. Rev. Appl.* **2018**, *10*, 064059. [CrossRef]
128. Awatani, T.; McQuillan, A.J. Adsorbed Thiosulfate Intermediate of Cadmium Sulfide Aqueous Photocorrosion Detected and Characterized by in Situ Infrared Spectroscopy. *J. Phys. Chem. B* **1998**, *102*, 4110–4113. [CrossRef]
129. de Tacconi, N.R.; Rajeshwar, K. Anodic Growth and Interphasial Photoelectrochemistry of Cadmium Sulfide Thin Films as Probed by Laser Raman Spectroscopy. *J. Phys. Chem.* **2002**, *97*, 6504–6508. [CrossRef]
130. Sourisseau, C.; Cruege, F.; Gorochov, O. In-Situ Raman Investigation of Photo-Corrosion Processes at p- and n-Type WS2 Electrodes in Acid Solutions. *J. Electroanal. Chem. Interfacial Electrochem.* **1991**, *308*, 239–253. [CrossRef]
131. Abshere, T.A.; Richmond, G.L. Picosecond Photoluminescence Study of the N-GaAs(100)/Methanol Interface in a Photoelectrochemical Cell. *J. Phys. Chem. B* **1999**, *103*, 7911–7919. [CrossRef]
132. Frese, K.W. Electrochemical Studies of Photocorrosion of n - CdSe. *J. Electrochem. Soc.* **1983**, *130*, 28. [CrossRef]
133. Lai, J.; Yuan, D.; Huang, P.; Zhang, J.; Su, J.-J.; Tian, Z.-W.; Zhan, D. Kinetic Investigation on the Photoetching Reaction of N-Type GaAs by Scanning Electrochemical Microscopy. *J. Phys. Chem. C* **2016**, *120*, 16446–16452. [CrossRef]
134. Zhang, S.; Ahmet, I.; Kim, S.-H.; Kasian, O.; Mingers, A.M.; Schnell, P.; Kölbach, M.; Lim, J.; Fischer, A.; Mayrhofer, K.J.J.; et al. Different Photostability of $BiVO_4$ in Near-PH-Neutral Electrolytes. *ACS Appl. Energy Mater.* **2020**, *3*, 9523–9527. [CrossRef] [PubMed]
135. Yi, S.-S.; Zhang, X.-B.; Wulan, B.-R.; Yan, J.-M.; Jiang, Q. Non-Noble Metals Applied to Solar Water Splitting. *Energy Environ. Sci.* **2018**, *11*, 3128–3156. [CrossRef]

136. Nguyen, V.-H.; Nguyen, T.P.; Le, T.-H.; Vo, D.-V.N.; Nguyen, D.L.; Trinh, Q.T.; Kim, I.T.; Le, Q. Van Recent Advances in Two-Dimensional Transition Metal Dichalcogenides as Photoelectrocatalyst for Hydrogen Evolution Reaction. *J. Chem. Technol. Biotechnol.* **2020**, *95*, 2597–2607. [CrossRef]
137. Eftekhari, A.; Babu, V.J.; Ramakrishna, S. Photoelectrode Nanomaterials for Photoelectrochemical Water Splitting. *Int. J. Hydrogen Energy* **2017**, *42*, 11078–11109. [CrossRef]
138. Bhat, S.S.M.; Jang, H.W. Recent Advances in Bismuth-Based Nanomaterials for Photoelectrochemical Water Splitting. *ChemSusChem* **2017**, *10*, 3001–3018. [CrossRef] [PubMed]
139. Naseri, A.; Samadi, M.; Pourjavadi, A.; Moshfegh, A.Z.; Ramakrishna, S. Graphitic Carbon Nitride (g-C_3N_4)-Based Photocatalysts for Solar Hydrogen Generation: Recent Advances and Future Development Directions. *J. Mater. Chem. A* **2017**, *5*, 23406–23433. [CrossRef]
140. Xiao, F.-X.; Miao, J.; Tao, H.B.; Hung, S.-F.; Wang, H.-Y.; Yang, H.B.; Chen, J.; Chen, R.; Liu, B. One-Dimensional Hybrid Nanostructures for Heterogeneous Photocatalysis and Photoelectrocatalysis. *Small* **2015**, *11*, 2115–2131. [CrossRef]
141. Benck, J.D.; Hellstern, T.R.; Kibsgaard, J.; Chakthranont, P.; Jaramillo, T.F. Catalyzing the Hydrogen Evolution Reaction (HER) with Molybdenum Sulfide Nanomaterials. *ACS Catal.* **2014**, *4*, 3957–3971. [CrossRef]
142. Ahmed, M.; Dincer, I. A Review on Photoelectrochemical Hydrogen Production Systems: Challenges and Future Directions. *Int. J. Hydrogen Energy* **2019**, *44*, 2474–2507. [CrossRef]
143. Pinaud, B.A.; Benck, J.D.; Seitz, L.C.; Forman, A.J.; Chen, Z.; Deutsch, T.G.; James, B.D.; Baum, K.N.; Baum, G.N.; Ardo, S.; et al. Technical and Economic Feasibility of Centralized Facilities for Solar Hydrogen Production via Photocatalysis and Photoelectrochemistry. *Energy Environ. Sci.* **2013**, *6*, 1983–2002. [CrossRef]
144. Shi, X.; Liao, X.; Li, Y. Quantification of Fresh Water Consumption and Scarcity Footprints of Hydrogen from Water Electrolysis: A Methodology Framework. *Renew. Energy* **2020**, *154*, 786–796. [CrossRef]
145. Shaner, M.R.; Atwater, H.A.; Lewis, N.S.; McFarland, E.W. A Comparative Technoeconomic Analysis of Renewable Hydrogen Production Using Solar Energy. *Energy Environ. Sci.* **2016**, *9*, 2354–2371. [CrossRef]
146. Grimm, A.; de Jong, W.A.; Kramer, G.J. Renewable Hydrogen Production: A Techno-Economic Comparison of Photoelectrochemical Cells and Photovoltaic-Electrolysis. *Int. J. Hydrogen Energy* **2020**, *45*, 22545–22555. [CrossRef]
147. Demir, M.E.; Chehade, G.; Dincer, I.; Yuzer, B.; Selcuk, H. Design and Analysis of a New System for Photoelectrochemical Hydrogen Production from Wastewater. *Energy Convers. Manag.* **2019**, *199*, 111903. [CrossRef]
148. Cha, H.G.; Choi, K.-S. Combined Biomass Valorization and Hydrogen Production in a Photoelectrochemical Cell. *Nat. Chem.* **2015**, *7*, 328–333. [CrossRef]
149. Nagarajan, S.; Skillen, N.; Robertson, P.; Lawton, L. Cellulose Photocatalysis for Renewable Energy Production. In *Metal, Metal-Oxides and Metal Sulfides for Batteries, Fuel Cells, Solar Cells, Photocatalysis and Health Sensors. Environmental Chemistry for a Sustainable World*; Springer: Berlin/Heidelberg, Germany, 2021; pp. 1–34. [CrossRef]
150. Rumayor, M.; Corredor, J.; Rivero, M.J.; Ortiz, I. Prospective Life Cycle Assessment of Hydrogen Production by Waste Photoreforming. *J. Clean. Prod.* **2022**, *336*, 130430. [CrossRef]